Performance Evaluation of Distributed Extended KDamper Devices for Seismic Protection of Mid-Rise Building Structures

Author(s):
Kapasakalis, Konstantinos; Mantakas, Antonios; Kalderon, Moris; Antoniou, Maria; Sapountzakis, Evangelos J.

Publication date:
2024

Permanent link:
https://doi.org/10.3929/ethz-b-000620176

Originally published in:
Journal of Earthquake Engineering 28(4), https://doi.org/10.1080/13632469.2023.2226227

Performance Evaluation of Distributed Extended KDamper Devices for Seismic Protection of Mid-Rise Building Structures

K. Kapasakalis [a]*, A. Mantakas[a], M. Kalderon[b], M. Antoniou[c], and E.J. Sapountzakis[a]

[a]*Institute of Structural Analysis and Antiseismic Research, School of Civil Engineering, National Technical University of Athens, Zografou Campus, GR-157 80 Athens, Greece*

e-mail: kostiskapasakalis@hotmail.com *, *mantakasantonis@gmail.com*, *cvsapoun@central.ntua.gr;*

[b]*Dynamics and Acoustics Laboratory, School of Mechanical Engineering, National Technical University of Athens, Zografou Campus, GR-157 80 Athens, Greece*

e-mail: moriska@mail.ntua.gr;

[c] *Institute for Geotechnical Engineering, Department of Civil, Environmental and Geomatic Engineering, ETH Zurich, Switzerland*

e-mail: maria.antoniou@igt.baug.ethz.ch;

Performance Evaluation of Distributed Extended KDamper Devices for Seismic Protection of Mid-Rise Building Structures

This study proposes a novel seismic protection strategy that applies and distributes extended KDamper devices (d-EKD) along the height of an existing mid-rise building structure. The performance of the d-EKD is assessed on a set of real earthquake records and is compared to a system with optimally distributed Tuned Mass Dampers (d-TMD). The proposed framework with the d-EKDs manages to outperform the d-TMDs, regardless the number of installed devices, further reducing the structure's dynamic responses by more than 15%, using 10 times lower total additional masses, rendering it a realistic and compelling alternative for passive seismic protection.

Keywords: Negative Stiffness; Seismic Protection; KDamper; Multiple Tuned Mass Dampers; Vibration Control Mechanism.

1. Introduction

During the latest years, structural damage and collapse of infrastructure and buildings due to severe earthquake excitation, has led to extensive research and alteration of seismic codes, aiming to achieve resilient structures with enhanced dynamic performance. The primary concern is to protect human lives as well as material content and maintain serviceability of the structural system. Mid and high-rise structures with large height-to-base ratio suffer from increased horizontal movement during earthquake excitation and consequently, are considered vulnerable to seismic motion (Naeim 1998). Current practice focuses on increasing structural mass, strength, and rigidity as well as ductility of crucial members of such structures, allowing in this way substantial inelastic behavior and increased damping. Permanent drifts and increased top storey accelerations, however, are unavoidable in the case of a relatively strong motion; the result is loss of serviceability, material and equipment damage, as well as potential degradation of the structural members. To this end, seismic isolation has been one of the

main approaches to decouple the superstructure from the foundation level and thus, protect the structure from the loads transferred during earthquake excitation (Farag, Mehanny, and Bakhoum 2015; Naeim and Kelly 1999; Symans et al. 2007; Warn and Ryan 2012). The main drawback of such approach is the required large base displacement and complex implementation, rendering the system expensive and inadequate for retrofitting of existing structures.

State-of-the-art in seismic protection includes the development of passive, active, semi-active, and hybrid energy dissipation and vibration control devices, which among others include shape memory alloys, (R. Kamgar, Heidarzadeh, and Babadaei Samani 2021; Mane and Kondekar 2021), steel infill plates, (Reza Kamgar and Samani 2021), adaptive string-mass systems (Acar and Yilmaz 2013) and more. The so-called Tuned Mass Damper (TMD) is considered perhaps the most popular and mature approach for passive vibration control. The TMD mechanism includes the incorporation of an additional oscillating mass attached to the primary structure, a stiffness element, as well as an additional damper. First introduced by Frahm (Frahm 1911) and optimized by Den Hartog (Den Hartog 1956), the TMD was designed for an undamped single-degree-of-freedom (SDOF) structure, subjected to harmonic excitation. Several researchers have employed the TMD in various structural systems and have reported significant improvements in their dynamic behavior (Dadkhah et al. 2020; De Domenico and Ricciardi 2018; Elias and Matsagar 2015; Hoang, Fujino, and Warnitchai 2008; Reza Kamgar et al. 2020; Reza Kamgar, Samea, and Khatibinia 2018; Kareem 1983; Kareem, Kijewski, and Tamura 1999; Khatibinia, Gholami, and Kamgar 2018; Salimi, Kamgar, and Heidarzadeh 2021; Taniguchi, Der Kiureghian, and Melkumyan 2008; Xiang and Nishitani 2014). However, even if the TMD has been widely studied and introduced in real life applications, it demonstrates two major drawbacks: (a) its

efficiency is highly dependent on the optimum frequency as well as the selected damping properties of the additional damper elements (Nagarajaiah and Sonmez 2007; Weber and Feltrin 2010) and (b) it requires heavy parasitic oscillating masses that occupy substantial space and burden the superstructure by generating additional static forces. In addition, research indicates that the use of a single TMD (STMD) for the seismic protection of buildings is not always efficient as earthquakes usually cover a broad spectrum of frequencies and consequently induce vibration not only in the fundamental but also in higher modes of building structures (Clark 1988; Sladek and Klingner 1983).

Aiming to overcome the disadvantages of single TMD systems, researchers have proposed the application of multiple TMDs (MTMDs), either placed at top floor or often distributed along different levels of a structure (d-MTMDs). Initially, Ayorinde and Warburton (1980) introduced the concept of MTMDs - already used in mechanical engineering - in civil engineering applications for seismic control. Within the years, optimization of the parameters of MTMDs, located at the top of the structure, has been studied by several researchers, indicating that these systems may be more efficient compared to the STMD, even for equal total additional mass (Abé and Fujino 1994; Igusa and Xu 1994; Kareem and Kline 1995; Suresh and Mini 2019; Xu and Igusa 1992; Yamaguchi and Harnpornchai 1993). The conclusion is that increasing the number of the optimized MTMDs, the control frequency bandwidth increases. The same applies for increase of the total additional mass of the dampers. Recently, research has been extended on the distribution of MTMDs spatially, not only to increase the efficiency of the system, but also to decrease the required concentrated additional mass that stresses the structure and occupies significant space. Chen & Wu (2001) studied the application of d-MTMDs on a six-storey structure subjected to seismic excitation.

Distribution was selected according to the acceleration modal response of the building. Xiang & Nishitani (2013) showcased that d-MTMDs are effective in earthquake vibration control of low-rise buildings with closely spaced eigen frequencies. Research has shown that distribution of the MTMDs and control of different modal responses based on the excitation frequency and eigenfrequencies of the structure leads to better structural performance compared to controlling only the fundamental modal response (Elias, Matsagar, and Datta 2016; Elias, Matsagar, and Datta 2017; Radmard Rahmani and Könke 2019).

Although the application of MTMDs for the mitigation of ground motion appears promising, the introduction of hefty oscillating masses to increase damping and consequently the performance of the vibration control system, remains an issue. As a consequence, amplification of the inertia and hence increase of the vibrational response of mechanical and structural systems is of key significance to achieve enhanced dynamic behavior and applicable damping technologies. Towards this direction, Smith et al. (Smith 2002) introduced the inerter, an innovative levered mass mechanism that takes advantage of the amplified inertia in order to achieve vibration control. Many research works have introduced the inerter and other amplification mechanisms as a means to enhance the performance of conventional dynamic systems and reduce mass requirements (Bhowmik and Debnath 2021; Cheng et al. 2020; Chowdhury, Banerjee, and Adhikari 2022; Jangid 2021; Kalderon et al. 2022; Kalderon, Mantakas, and Antoniadis 2023; Kalderon, Paradeisiotis, and Antoniadis 2021; Konstantinos A. Kapasakalis, Antoniadis, and Sapountzakis 2021b; Paradeisiotis, Kalderon, and Antoniadis 2021). In Marian & Giaralis (Marian and Giaralis 2014) and Giaralis & Taflanidis (Giaralis and Taflanidis 2018) an inerter-enhanced TMD has been proposed. This Tuned Mass Damper Inerter (TMDI) incorporates an inertance element that

introduces an apparent increase of the damper's inertia without any addition to its actual mass. Very recently, Chen et al. (2022) evaluated the performance of multiple tuned inerter-based dampers for seismic vibration control.

Apart from the existing inerter based methodologies, the introduction of negative stiffness (NS) elements has been proposed as an artificial way to increase the inertia of oscillators and to improve the dynamic response of traditional TMDs. Antoniadis et al. (Antoniadis et al. 2018) have proposed the KDamper, a novel passive NS-based absorber that is based on the combination of stiffness, mass and damping elements, including a negative stiffness element. The incorporation of the NS element achieves an enhanced dynamic behavior of the oscillating mass of a TMD, leading to extraordinary damping properties without the need of additional heavy parasitic masses. The concept has been applied in various vibration control applications, such as seismic mitigation of bridges, buildings and wind turbines (Andreas et al. 2020; Kampitsis, Kapasakalis, and Via-Estrem 2022; K.A. Kapasakalis, Antoniadis, and Sapountzakis 2020; K. Kapasakalis, Antoniadis, and Sapountzakis 2019; Konstantinos A. Kapasakalis, Antoniadis, and Sapountzakis 2022; Syrimi et al. 2017). The influence of spatially varying ground motions (SVGMs) was studied by Jiang et al. (Jiang et al. 2023) to the response of large-spanning bridges equipped with KDampers, revealing that the KDamper effectiveness is more evident when SVGMs are considered, compared to the uniform ground motions, and should be considered when large structures are investigated (Emami and Tayefeh Mohammad Ali 2022). Kapasakalis et al. (K.A. Kapasakalis, Antoniadis, and Sapountzakis 2021), introduced an extended version of the KDamper, namely the EKD, to mitigate vibration of low-rise buildings due to earthquake excitation. In addition, Mantakas et al. (Mantakas et al. 2022) have introduced and optimized the EKD device as a means of seismic retrofitting of existing

residential buildings, by applying the concept between the foundation and the superstructure. Finally, an extended work has been conducted in terms of the optimization of the KDamper devices aiming for the minimization of the structural accelerations while ensuring static structural integrity, increased damping capabilities and the containment of the relative base displacements (static and dynamic) both for vertical (M. Kalogerakou, Paradeisiotis, and Antoniadis 2023; M. E. Kalogerakou et al. 2023; Konstantinos A. Kapasakalis, Antoniadis, and Sapountzakis 2021a) and horizontal excitations (K.A. Kapasakalis, Antoniadis, and Sapountzakis 2021; Konstantinos A. Kapasakalis, Antoniadis, and Sapountzakis 2021b), respectively.

In this paper, the EKD is extended and applied to multiple floors of an existing mid-rise 10-storey benchmark building, inspired by the MTMDs concept. More specifically, a number of EKDs are installed and distributed (d-EKDs) along the height of the aforementioned structure, and aim to seismically protect it in terms of floor absolute accelerations, floor displacements, floor drifts and total base shear. In order to avoid burdening the building with large parasitic masses, which is the main disadvantage of all mass related vibration control approaches (TMDs, KDampers, etc.), the design of the d-EKDs foresees significantly small total additional masses. The spatial allocation and optimal parameters of the distributed devices are obtained following a constrained optimization approach based on a Harmony Search (HS) algorithm, with proper constraints and limitations imposed by the structure as well as the constructability of the system. In addition, static and dynamic stability conditions are imposed in the optimization procedure, to ensure the stability of the examined structure, as the d-EKD concept introduces negative stiffness (NS) elements. A database of Eurocode 8 compatible artificial accelerograms is generated and introduced as input to the optimization process in order to obtain optimal EKD parameters for the

benchmark structure. Finally, the performance of the controlled benchmark building with the d-EKDs is assessed on a set of performance criteria for the dynamic responses, evaluated for a set of real earthquake records and is compared to a controlled structure with optimally designed d-TMDs.

The novelties of the proposed vibration control approach in this research work are summarized as follows:

(1) A novel passive retrofitting strategy is proposed for the seismic protection of mid-rise building structures.
(2) The proposed d-EKD design is based on a constrained optimization approach based on engineering criteria and accounts for constraints and limitations imposed by the structure.
(3) The NS elements are realized by articulated mechanisms that employ conventional positive stiffness elements. In addition, a variation in the value of the generated NS is foreseen, and static and dynamic stability conditions are imposed in the d-EKD design to ensure the stability of the examined structure.
(4) The implemented passive seismic protection devices do not burden the structure with large parasitic masses, and do not weaken the building structure or significantly alter its structural properties, even though the d-EKD introduced additional masses and NS elements.

The key features of the d-EKD design implemented in the benchmark building, as compared to the original structure and a controlled one with optimally designed d-TMDs are the following:

(1) Based on the numerical results obtained, the d-EKD retrofitting strategy, as compared to an optimally designed d-TMD concept, outperforms the d-TMD in

reducing the structural dynamic responses for all the artificial and real earthquake excitations.

(2) The total added oscillating masses introduced by the d-EKD approach is one order of magnitude lower than that of the d-TMDs.

(3) The stiffness and damping parameters of the implemented devices are in realistic ranges, as the optimization procedure followed for the design of the d-EKDs accounts for limitations imposed by the constructability of the system.

2. Mathematical Modeling

In this study, a ten-storey shear frame structure with uniform mass and stiffness for all storeys, taken from Singh et al. (Singh, Matheu, and Suarez 1998) is considered. The structure represents a typical medium-sized multi-storey building whose floor weights correspond to about 400 m^2 of floor area. The assumptions made for the analytical formulation are: (*i*) the structure is considered to remain within the elastic limit under earthquake excitations, (*ii*) the building is subjected to a single horizontal (uni-directional) component of the ground motion, and (*iii*) the effects of soil-structure-interaction are not taken into consideration. The building parameters (mass and stiffness of each floor) have been slightly modified as in Hadi and Arfiadi (Hadi and Arfiadi 1998). The mass of each storey is equal to M_F = 360 *tn*, the stiffness of each storey is k_F =650 *MN/m*, and the height of each storey is assumed 3.2 *m*. A schematic representation of the examined multi-storey building structure, along with the lumped mass dynamic model and the first five natural modes is presented in Figure 1.

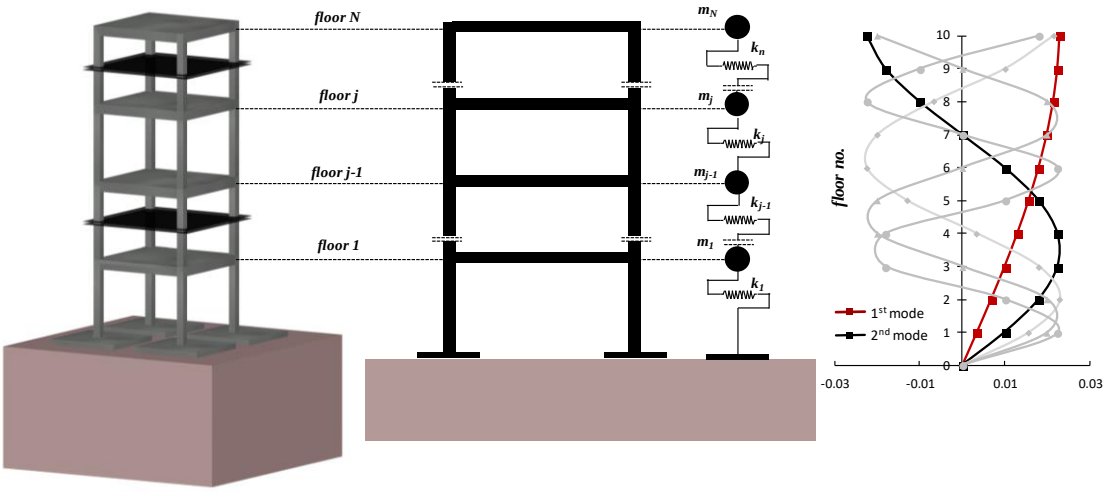

Figure 1. Schematic representation of the examined multi-storey building structure, the lumped mass dynamic model, and the first five eigen forms.

The N degrees of freedom (DoF) benchmark building (N=10 in our case) is installed with n number of dynamic vibration absorption (DVA) devices (TMDs, KDampers, EKDs, etc.), thereby, the total DoFs of the controlled system with the DVAs becomes (N+n). In general, the governing equations of motion of the structure installed with the DVAs are obtained by considering the equilibrium of forces at the location of each DoF (structural floors and installed devices) as follows:

$$[M]\{\ddot{X}\}+[C]\{\dot{X}\}+[K]\{X\}=-[M]\{r\}\ddot{X}_G \tag{1}$$

where $[M]$, $[C]$, and $[K]$ are the mass, damping, and stiffness matrices of the controlled structure, respectively, considering the effect of the implemented DVAs. These matrices are defined as:

$$[M]=[M_{STR}]+[M_{DVA}] \tag{2.a}$$

$$[C] = [C_{STR}] + [C_{DVA}] \tag{2.b}$$

$$[K] = [K_{STR}] + [K_{DVA}] \tag{2.c}$$

Indexes *STR* and *DVA* in Eq. (2.a-c) indicate the DoFs of the NC (no-control) building structure and of the implemented DVAs, respectively. Further details regarding the matrices related to the NC shear building, modelled as a lumped mass system, as well as the vectors introduced in Eq. (1) can be found in Appendix A.

Modal analysis is conducted to determine the natural frequencies, mode shapes, and modal mass participation factors of the original NC building. The natural frequencies of the 10-storey benchmark structure are determined to be: $[f_i] = [1.01,\ 3.01,\ 4.94,\ 6.76,\ 8.43,\ 9.91,\ 11.17,\ 12.19,\ 12.92,\ 13.37]$ Hz. In Figure 1 the first five natural modes are presented. Only the first two (2) modes are presented in bold, as they predominantly influence the total dynamic response of the NC structure, having a sum of modal mass participation factors equal to ninety percent or more. The damping matrix is defined under the assumption of modal damping. The damping ratio in each mode is assumed to be proportional to the frequency of the associated structural mode of the NC building, with a maximum of 10% critical damping in any vibration mode. The damping ratio of the first mode f_1 (fundamental) is assumed to be $\zeta_1 = 3.03\%$ (Etedali and Rakhshani 2018). Therefore, damping of the i^{th} mode is given by:

$$\zeta_i = \min\left\{\zeta_1 \frac{\Omega_i}{\Omega_1},\quad 0.1\right\} \tag{3}$$

The damping matrix of the NC structure is thus defined as:

$$[C_{STR}] = [M_{STR}][\Phi_{STR}] \begin{bmatrix} 2\zeta_1\Omega_1 & 0 & \cdots & 0 \\ 0 & 2\zeta_2\Omega_2 & \cdots & 0 \\ \vdots & \vdots & \ddots & \vdots \\ 0 & 0 & \cdots & 2\zeta_N\Omega_N \end{bmatrix} [\Phi_{STR}]^T [M_{STR}] \quad (4)$$

where $[\Phi_{STR}]$ is the matrix of the modal shapes.

3. Proposed Retrofitting Strategy with Distributed Extended KDampers

Seismic isolation is considered perhaps the most popular approach to earthquake-resistant design (Naeim and Kelly 1999). However, the large required base displacements prohibit retrofitting. Increasing the damping of the base isolated system, to reduce displacements (Symans et al. 2007), cannot be considered as a mainstream alternative due to the technological requirements and the subsequent increase of the inter-storey drifts and floor accelerations (Kelly 1999). As a result, alternative vibration absorption devices have been developed and investigated for seismic retrofitting of existing structures. One of the most popular passive retrofitting strategies for seismic protection is the use of a single TMD (STMD). However, the use of an STMD is not always effective as real ground motions usually have a broad frequency content and consequently induce vibration not only in the fundamental but also in higher modes of building structures (Clark 1988; Sladek and Klingner 1983). To this aim, the application of multiple TMDs (MTMDs), either placed at top floor or often distributed along different levels of a structure (d-MTMDs) is examined, in order to increase the frequency bandwidth of the retrofitting strategy. Even though the implementation of MTMDs appears promising, introducing multiple heavy oscillating masses remains an issue. For this reason, in this paper we examine the installation of multiple distributed EKD devices, as previous research (K.A. Kapasakalis, Antoniadis, and Sapountzakis 2020; K.A. Kapasakalis, Antoniadis, and Sapountzakis 2021) indicates that KDamper-

based designs present an overall superior dynamic behavior over TMD related configurations, with significantly less additional masses. A schematic representation of the installation of an EKD (or a TMD) device number (*i*) between the floors (*j*) and (*j-1*) is illustrated In Figure 2. In the following paragraphs, the analytical procedure of the installation of a DVA (EKD or TMD) is presented, along with the modification of the property matrices of Eqs. (2) that account for such DVAs.

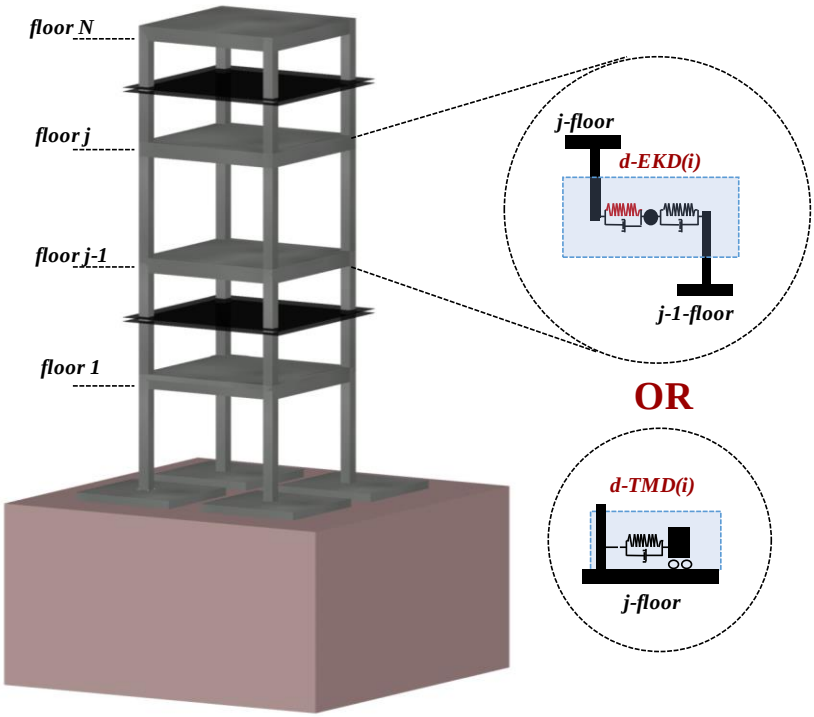

Figure 2. Implementation of a DVA number (i) (Tuned Mass Damper – TMD or extended KDamper – EKD) between the floors (j) and (j-1) of the N-storey building structure.

For each EKD number (*i*) installed between the floors (*j*) and (*j-1*), as presented in Figure 2, the additional oscillating mass $M_{D\text{-}i}$ is attached to the floor (*j*) with a negative stiffness element $k_{N\text{-}i}$ and an artificial damper $c_{N\text{-}i}$, as well as to the floor (*j-1*) with a positive stiffness element $k_{P\text{-}i}$ and an artificial damper $c_{P\text{-}i}$. The property matrices that account for such an EKD can be formed as follows:

$$K_{DVA}(N+i,N+i)=k_{N-i}+k_{P-i} \tag{5.a}$$

$$K_{DVA}(N+i,j)=-k_{N-i} \tag{5.b}$$

$$K_{DVA}(j,N+i)=-k_{N-i} \tag{5.c}$$

$$K_{DVA}(j,j)=k_{N-i} \tag{5.d}$$

$$K_{DVA}(N+i,j-1)=-k_{P-i} \tag{5.e}$$

$$K_{DVA}(j-1,N+i)=-k_{P-i} \tag{5.f}$$

$$K_{DVA}(j-1,j-1)=k_{P-i} \tag{5.g}$$

$$M_{DVA}(N+i,N+i)=\mu_i M_{TOT} \tag{6}$$

$$\mu_i=\frac{M_{D-i}}{M_{TOT}} \tag{7.a}$$

$$\mu=\sum_{1}^{n}\mu_i \tag{7.b}$$

$$M_{TOT}=\sum_{1}^{N}M_i \tag{8}$$

$$C_{DVA}(N+i,N+i)=c_{N-i}+c_{P-i} \tag{9.a}$$

$$C_{DVA}(N+i,j)=-c_{N-i} \tag{9.b}$$

$$C_{DVA}(j,N+i)=-c_{N-i} \tag{9.c}$$

$$C_{DVA}(j,j)=c_{N-i} \tag{9.d}$$

$$C_{DVA}(N+i,j-1)=-c_{P-i} \tag{9.e}$$

$$C_{DVA}\left(j-1, N+i\right) = -c_{P-i} \tag{9.f}$$

$$C_{DVA}\left(j-1, j-1\right) = c_{N-i} \tag{9.g}$$

where μ_i is the mass ratio of each EKD number (i), defined in Eq. (7.a) and is expressed as a percentage of the total superstructure mass M_{TOT}, defined in Eq. (8), and μ is the total mass ratio of all the installed EKD devices, as defined in Eq. (7.b). To verify the effectiveness of the d-EKD retrofitting strategy, the existing structure is also examined with distributed TMD devices (Elias, Matsagar, and Datta 2016; Elias, Matsagar, and Datta 2017; Sladek and Klingner 1983; Xiang and Nishitani 2013). Further details regarding the property matrices that account for d-TMDs are presented in Appendix B.

4. Optimal Design of the d-EKD

The optimum design of most vibration control approaches is strongly dependent on the tuning of the installed devices and the implemented damping ratios of the artificial dampers. Numerous approaches have been proposed in the literature for the selection of the optimal system parameters (Abé and Fujino 1994; Bakre and Jangid 2007; Fahim et al. 1998; Hoang, Fujino, and Warnitchai 2008; C. Li 2002; Warburton 1982; Zuo, Bi, and Hao 2017). However, the complexity and the number of the design variables of the d-EKD DVA concept renders the conventional min-max $H\infty$ approaches (Den Hartog 1956) ineffective.

The parameters of the EKD are evaluated using constrained Optimization Algorithms (K.A. Kapasakalis, Antoniadis, and Sapountzakis 2021), as it is an efficient approach to design effective and practical devices for vibration mitigation. The Harmony Search (HS) algorithm, a novel metaheuristic algorithm is employed (Zong Woo Geem, Joong Hoon Kim, and Loganathan 2001). The parameters inherently

involved in the HS algorithm, are selected according to relative literature, and are *HMS*=75, *HMCR*=0.5, and *PAR*=0.1. Details regarding the design variables, dependent and independent, are provided in the following subsections.

4.1 Negative Stiffness and Stability Esurance

Since the proposed vibration control strategy includes negative stiffness elements, it is necessary to ensure that the controlled system will remain statically and dynamically stable. For an EKD number (*i*) installed between the floors (*j*) and (*j-1*), the equivalent static stiffness of the (*j*) floor is obtained from the following equation:

$$k_{EQ,STAT}^{j} = k_F + \frac{k_{N-i} \times k_{P-i}}{k_{N-i} + k_{P-i}} \tag{10}$$

where k_F is the original stiffness of the (*j*) floor. Although theoretically the value of the NS element k_{N-i} is assumed to be constant, manufacturing tolerances and non-linear behaviors may present variations in practice, as almost all negative stiffness designs result from unstable non-linear systems (H. Li, Li, and Li 2020). In order to ensure the dynamic stability of the controlled structure, the variation of the k_{N-i} is accounted for by introducing the variation factor V_{N-i} in Eq. (11):

$$k_{EQ,DYN}^{j}\left(V_{N-i}\right) = k_F + \frac{V_{N-i}k_{N-i} \times k_{P-i}}{V_{N-i}k_{N-i} + k_{P-i}} \tag{11}$$

Thus, two parameters are introduced as stability conditions (SC) (static and dynamic) and are defined as the stiffness ratio, between the equivalent stiffness of the (*j*) floor over the initial value of the NC building structure:

$$SC_{STAT}^{j} = \frac{k_{EQ,STAT}^{j}}{k_F} \tag{12}$$

$$SC_{DYN}^{j} = \frac{k_{EQ,DYN}^{j}\left(V_{N-i}\right)}{k_F} \tag{13}$$

In this work, the negative stiffness element is realized with a mechanical configuration that implements conventional pre-compressed springs and an articulated mechanism. Further information regarding the analytical design procedure can be found in Antoniadis (Antoniadis et al. 2018). The value of the V_{N-i} parameter is selected to be equal to 1.1 (+10%) and accounts for both manufacturing tolerances and non-linearities due to the non-linear behavior of the NS mechanism, as in Kapasakalis (K.A. Kapasakalis, Antoniadis, and Sapountzakis 2021) it is proven that by properly selecting the NS configuration parameters, the generated NS is close to constant. More specifically, the NS element k_{N-i} is realized with a mechanical configuration that incorporates a single conventional positive stiffness element which connects the additional oscillating mass with the floor (j), using an articulated mechanism (Antoniadis et al. 2018; K.A. Kapasakalis, Antoniadis, and Sapountzakis 2021). The proposed device is schematically presented in Figure 3a. The generated NS of this design is given by:

$$k_{N-i} = -k_{N-i,POS}\left(1+\frac{c_{I-i}}{\left(1-\left(\frac{X_{N-i}}{a_{N-i}}\right)^2\right)^{3/2}}\right) \tag{14}$$

$$X_{NS-i} = X_{STR-j} - X_{EKD-i} \tag{15}$$

where c_{I-i} is a non-dimensionalized design variable that correlates the constant

geometric properties of the mechanism, and $a_{N\text{-}i}$ is the rod length of the articulated mechanism. $X_{N\text{-}i}$ is the NS stroke, defined as the relative displacement between the NS terminals of the EKD number (i) installed between the floors (j) and (j-1) (the additional mass $M_{D\text{-}i}$ is attached to the floor (j) with the NS element $k_{N\text{-}i}$). $k_{N\text{-}i,POS}$ is the required conventional positive stiffness in order to generate the desired NS $k_{N\text{-}i}$. The NS mechanism is illustrated in Figure 3 in its initial equilibrium position, as well as in a randomly deformed state.

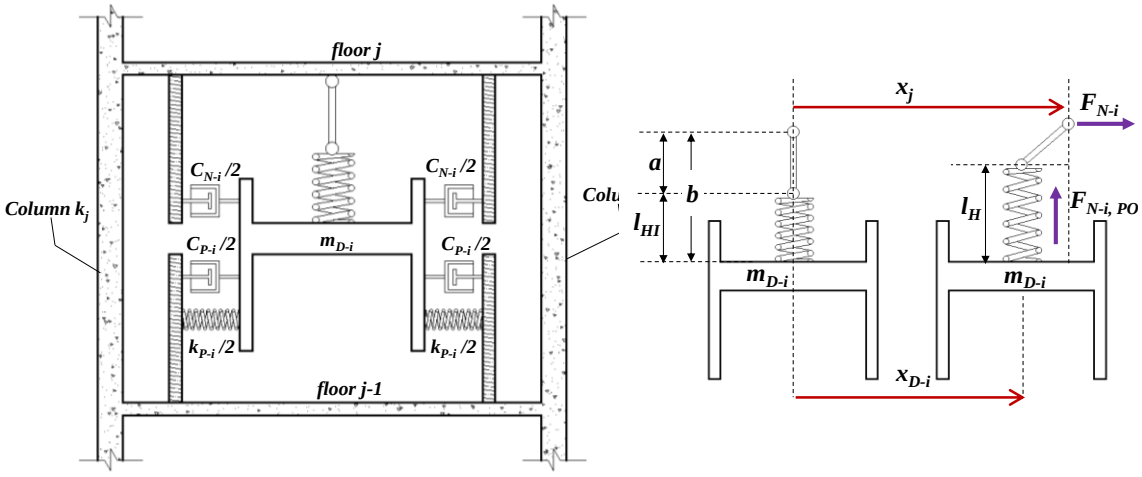

(a) (b)

Figure 3. (a) Conceptual representation of the EKD device, installed between floors (j) and (j-1), and (b) detailed sketch and annotation of the envisaged negative stiffness mechanism.

4.2 Dependent and Independent Design Variables

Each EKD number (i) introduces in total five additional parameters-elements, the oscillating mass $M_{D\text{-}i}$, the stiffness elements $k_{N\text{-}i}$ and $k_{P\text{-}i}$, and the artificial dampers $c_{N\text{-}i}$ and $c_{P\text{-}i}$. In order to avoid adding large parasitic masses in the structure, as in the d-TMD concept, the additional mass of each EKD is selected to be equal to 0.1% of the total structural mass M_{TOT}, Eq. (8). In addition, the equivalent frequency of the (j) floor is introduced to better observe the effect of the installed EKD device in the structural

system:

$$\omega_{EQ}^{j} = 2\pi f_{EQ}^{j} = \sqrt{\frac{k_{EQ,STAT}^{j}}{\left(M_j + M_{D-i}\right)}} \tag{16}$$

As a result, the value of the positive stiffness element $k_{P\text{-}i}$, assuming that the value of the NS element $k_{N\text{-}i}$ is known, can be obtained from Eq. (16). The artificial damper $c_{N\text{-}i}$ and $c_{P\text{-}i}$ can be expressed with respect to their damping ratios as follows:

$$c_{N-i} = 2\zeta_{N-i}\left(M_j + M_{D-i}\right)\omega_{EQ}^{j} \tag{17.a}$$

$$c_{P-i} = 2\zeta_{P-i}\left(M_j + M_{D-i}\right)\omega_{EQ}^{j} \tag{17.b}$$

Thus, the free (independent) design variables of the d-EKD system are ($4\times n$) in total. These are the following:

(1) The value of the NS element $k_{N\text{-}i}$. ($\times n$)

(2) The value of the equivalent frequency f_{EQ}^{j}. ($\times n$)

(3) The value of the artificial dampers $c_{N\text{-}i}$ and $c_{P\text{-}i}$ (or equivalently $\zeta_{N\text{-}I}$, $\zeta_{P\text{-}i}$). ($\times 2n$)

4.3 Optimization Process, Manufacturing Constrains and Limitations

Having established the equations of motion Eqs. (1) for the controlled building structure with distributed EKD (d-EKD) devices, the next objective is to determine the optimal d-EKD parameters in order to attain the best possible passive retrofitting strategy. For the design to be efficient and realistic as possible, proper constraints regarding the structural dynamic response, as well as limitations to the design variables must be applied:

(1) The controlled structure's maximum (absolute value) drift is set as the objective function.

(2) Since the d-EKD concept considers distributed EKD devices along the height of the structure, a small additional mass of 0.1% for each device is selected in order to avoid burdening the structure with parasitic masses (Konstantinos A. Kapasakalis, Antoniadis, and Sapountzakis 2021b).

(3) The position of the EKD number (i) device varies from 1:N, where N is the number of floors (N=10).

(4) The input motion in the optimization procedure is selected from a database of artificial accelerograms (K.A. Kapasakalis, Antoniadis, and Sapountzakis 2021) (30 in total), designed to be spectrum-compatible with the EC8 acceleration response spectrum.

(5) The static and dynamic stability of the structure is ensured by imposing a conservative lower limit to the non-dimensionalized stability-condition parameters:

$$SC_{STAT}^{j} \geq 0.5 \tag{18}$$

$$SC_{DYN}^{j} \geq 0.2 \tag{19}$$

(6) The (absolute) value of the NS element and the NS stroke are constrained with an upper limit based on Kapasakalis et al. (Konstantinos A. Kapasakalis, Antoniadis, and Sapountzakis 2021b):

$$\left|k_{N-i}\right| \leq 50 \quad kN/m/tn \tag{20}$$

$$X_{NS-i} \leq 0.18 \quad m \tag{21}$$

(7) The damping ratio of the artificial dampers has an uuper bound based on previous research work (K.A. Kapasakalis, Antoniadis, and Sapountzakis 2021) and manufacturing restrictions:

$$\zeta_{N-i},\ \ \zeta_{P-i} \le 20 \quad \% \tag{22}$$

(8) The equivalent frequency of the (*j*) floor is selected to vary in the range:

$$\left(2/3\right)\times\sqrt{\frac{k_F}{M_F}} \le \omega_{EQ}^{j} = 2\pi f_{EQ}^{j} = \sqrt{\frac{k_{EQ,STAT}^{j}}{\left(M_F + M_{D-i}\right)}} \le \left(4/3\right)\times\sqrt{\frac{k_F}{M_F}} \tag{23}$$

where k_F and M_F are the stiffness and mass of the j^{th} floor, respectively. This range is selected to avoid significant alterations in the structural properties, and thus endanger the stability of the building. The design process as well as the manufacturing constrains and limitations for a realistic and optimized design are depicted in the flowchart of Figure 4.

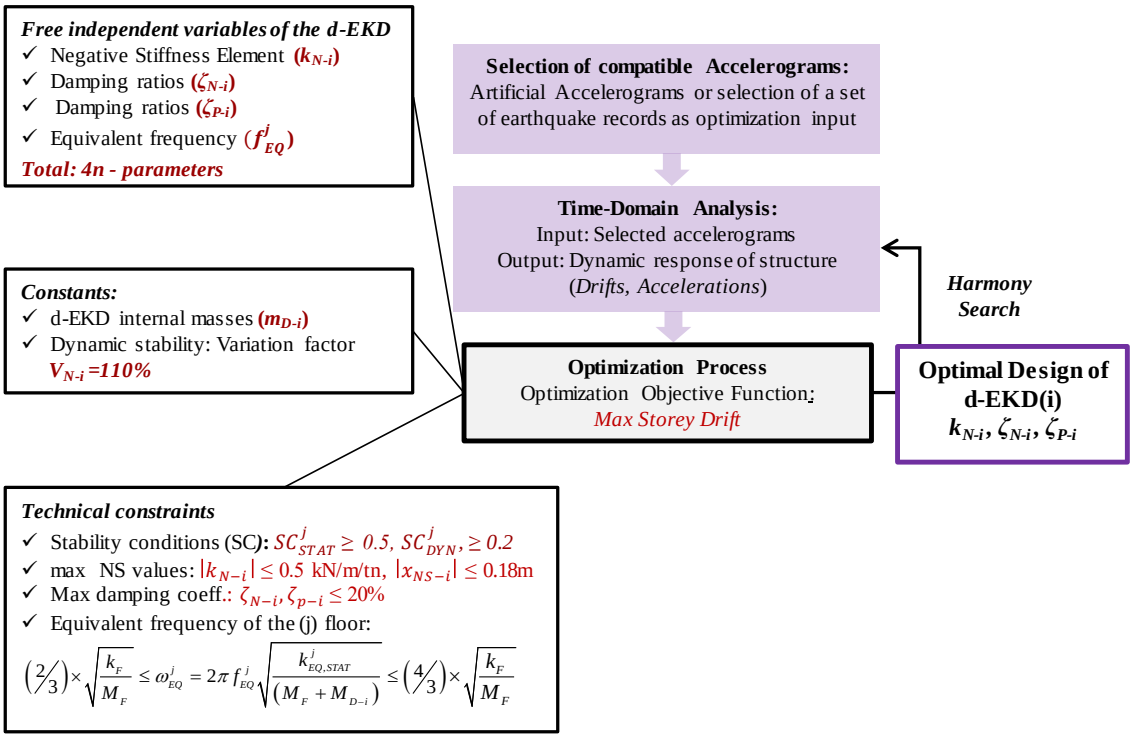

Figure 4. Flowchart briefly presenting the design and optimization process of the d-EKD components.

4.4 Distributed TMD (d-TMD) Design

The effectiveness of installing multiple distributed TMDs in a building depends on the total mass ratio $\mu = \sum_{1}^{n} \mu_i$, where n is the total number of implemented TMDs, between the total added mass of the TMDs, and the total mass of the building, M_{TOT} (Eq. (8). The deciding criterion for the number of the TMDs to be installed, as in Elias et al. (Elias, Matsagar, and Datta 2017), requires that the modal mass participation is greater than 90%, resulting in vibration control of the first two modal responses. An additional TMD that controls the 3rd mode is implemented to examine if further devices manage to increase the effectiveness of the d-TMD control strategy. The tuning frequency ratio of each TMD is calculated such that:

$$t_{TMD-i} = \frac{\omega_{TMD-i}}{\Omega_i}, \quad i = 1:n, \quad n = 3 \tag{24}$$

where $\omega_{TMD\text{-}i}$ is the tuning frequency of the TMD number (i), and Ω_i is the eigenfrequency of the i^{th} mode of the NC building structure to be controlled. The tuning frequency of the TMD number (i) is expressed as follows:

$$\omega_{D-i}^2 = \left(2\pi f_{D-i}\right)^2 = \frac{k_{D-1}}{M_{D-i}} \tag{25}$$

The optimum tuning frequency ratios $\left(t_{TMD-i}^{opt},\ i = 1:n\right)$ are calculated for a base excited building structure based on the formula given by Elias et al. (Elias, Matsagar, and Datta 2017):

$$t_{TMD-i}^{opt} = \frac{1}{1+\mu_i\varphi_i}\left(1-\zeta i\sqrt{\frac{\mu_i\varphi_i}{1+\mu_i\varphi_i}}\right), \quad i = 1:n, \quad n = 3 \tag{26}$$

where μ_i is the mass ratio of the TMD number (i), ζ_i is the damping ratio of the i^{th} mode of the structure, and φ_i is the amplitude of the first mode of vibration for a unit modal participation factor computed at the location of the TMD (i). The damping ratio of the TMD (i) device is obtained from the following equation, as provided by Elias et al. (Elias, Matsagar, and Datta 2017):

$$\zeta_{TMD-i}^{opt} = \varphi_i\left(\frac{\zeta_i}{1+\mu_i} + \sqrt{\frac{\mu_i}{1+\mu_i}}\right), \quad i = 1:n, \quad n = 3 \tag{27}$$

Finally, the value of the artificial damper is calculated as:

$$c_{D-i} = 2\zeta_{TMD-i}^{opt} M_{D-i}\omega_{D-i}^{opt} \tag{28}$$

5. Numerical Study

An analytical framework is developed aiming to calculate reliably the seismic

performance of the uncontrolled structural system and compare it with the performance of the system with the d-TMDs and the d-EKDs. To this end, design and optimization of the d-EKD parameters is undertaken based on the framework described in section 4. Three different systems are studied herein: a) a system with 1-EKD, b) 2-EKDs, c) 3-EKDs. The parameters of the devices as well as their spatial allocation along the height of the building are selected according to the HS optimization algorithm. A corresponding system upgraded with a) 1-TMD, b) 2-TMDs and c) 3-TMDs is generated and designed based on the analytical solutions provided by Elias (Elias, Matsagar, and Datta 2017). Time-history analyses are subsequently undertaken for the generated 30 artificial accelerograms and the dynamic behavior of the different systems in terms of accelerations, inter-storey drifts and absolute displacements is assessed.

5.1 Design and Optimization Results

Optimization of the d-EKD proposed framework has been conducted by adopting the HS optimization algorithm and 30 artificial, Eurocode 8 compatible, accelerograms. Optimal parameters and spatial allocation of the mechanisms on the benchmark structure considering one, two and three installed devices, distributed along the height of the building are provided in Table 1. In addition, the corresponding d-TMD optimized parameters are presented in Table **2**.

Figure 5 presents the first three natural modes of the NC structure, as well as the natural modes of the controlled building with distributed 3-TMDs and 3-EKDs, respectively. Results depict minimal effect of the vibration control systems on the modes of the structure, indicating no significant alteration of the structural properties and eigenfrequencies due to the installation of the vibration control devices, despite the addition of masses and negative stiffness elements.

Figure 6-8 present the envelopes of the relative to the ground displacements of each storey, inter-storey drifts for each level, as well as absolute accelerations for the 30 artificial accelerograms. A comparison between the dynamic response of the uncontrolled structure and the response of the upgraded building with d-TMDs and d-EKDs is depicted herein.

Specifically, Figure 6 illustrates a significant reduction of the storey displacements for the cases of the controlled buildings with d-TMDs and d-EKDs, respectively. A decrease of approximately 34% of the upper-storey displacements is indicated for the case of the d-TMDs (Figure 6a). However, minimal enhancement of the performance is observed as the number of TMDs increases. On the contrary, as the number of the d-EKD devices increases, a clear improvement of the superstructure's response is observed; for the case of 3-EKDs, a dramatic upper-storey displacement reduction of approximately 47% is achieved (Figure 6b). In Figure 6c, a comparison between the relative to the ground displacements for the building with 3-EKDs, 3-TMDs and the original uncontrolled structure is presented, showcasing the superiority of the d-EKD concept.

Similar behaviour is observed for the case of inter-storey drifts (Figure 7). Both d-TMD and d-EKD systems demonstrate an enhanced behaviour compared to the original structure; the system with 3-EKDs presents a first-storey drift reduction of approximately 47% while the system with 3-TMDs a decrease of approximately 30%. Once again, a superior behaviour of the d-EKD system is observed as the number of EKDs increases (Figure 7b) while the number of TMD devices displays minimal effect on the response of the structure (Figure 7a). However, a slight increase of the 5th-storey drifts is presented for the case of the d-EKDs, at the location of the first EKD device. This is attributed to the decrease of the floor's stiffness, resulting to a relatively softer

localized behaviour, leading to a higher displacement demand. Nonetheless, in terms of inter-storey drifts, the d-EKD system still outperforms both the original structure and the d-TMD upgraded building (Figure 7c).

Finally, Figure 8 demonstrates results of all storey accelerations, for the 30 artificial accelerograms. Results indicate the improved performance of the d-EKDs compared to the original structure and the system with the d-TMDs, showcasing that significant vibration mitigation is achieved by adopting such a vibration control system with minimal additional masses, compared to the d-TMD approach. Specifically, the system with 3-EKDs presents a top-storey acceleration decrease of approximately 43% while the system with 3-TMDs displays a top-storey acceleration decrease equal to approximately 32%.

Table 1 Optimal parameters of the d-EKD concept considering one, two, and three installed devices.

System	#Device/floor	k_{N-i}/k_F (%)	k_{P-i}/k_F (%)	f_{EQ}^{j} (Hz)	ζ_{N-i} (%)	ζ_{P-i} (%)	μ_i (%)
1-EKD	#1/floor 5	-0.122	0.162	4.78	0.136	0.023	0.1
2-EKDs	#1/floor 5	-0.121	0.160	4.79	0.137	0.023	0.1
	#2/floor 4	-0.096	0.123	4.99	0.131	0.022	0.1
3-EKDs	#1/floor 5	-0.127	0.171	4.78	0.137	0.023	0.1
	#2/floor 4	-0.104	0.133	4.92	0.133	0.022	0.1
	#3/floor 3	-0.085	0.106	5.10	0.129	0.021	0.1

Table 2 Optimal parameters of the d-TMD concept considering one, two, and three installed devices.

System	#Device/floor	f_{TMD-i}^{opt} (Hz)	ζ_{TMD-i}^{opt} $(\%)$	μ_i $(\%)$
1-TMD	#1/floor 10	0.998	12.95	1
2-TMDs	#1/floor 10	0.998	12.95	1
	#2/floor 4	2.9726	10.67	1
3-TMDs	#1/floor 10	0.998	12.95	1
	#2/floor 4	2.9726	10.67	1
	#3/floor 6	4.859	15.56	1

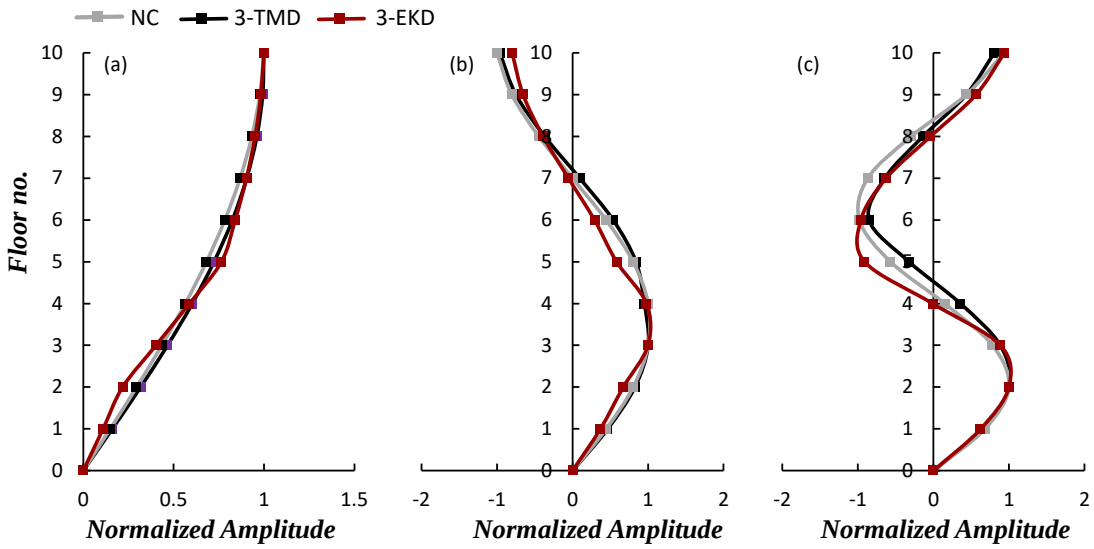

Figure 5. First three natural modes of the NC structure, as well as the controlled building with distributed 3-TMDs and 3-EKDs, respectively.

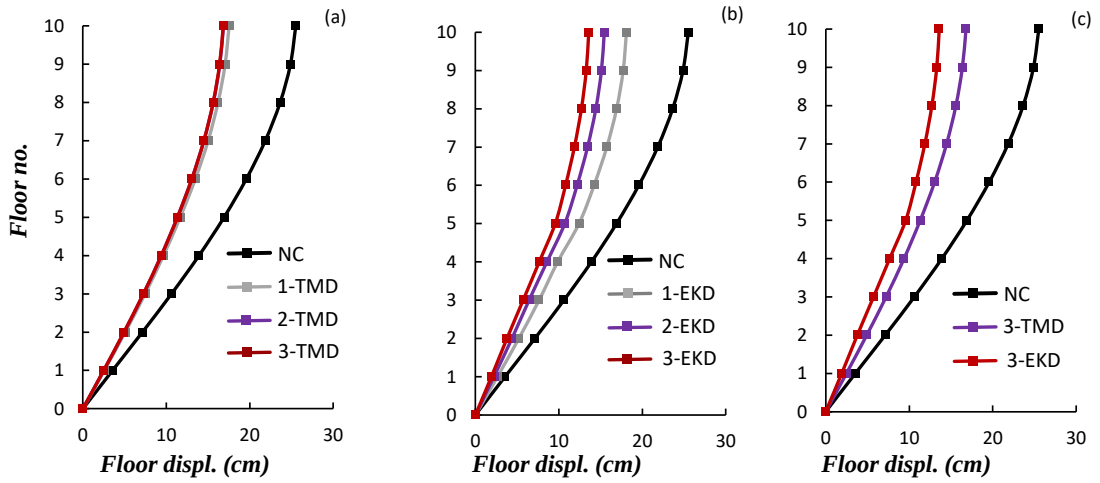

Figure 6**.** Relative to the ground floor displacement envelopes, for the (a) d-TMDs, (b) d-EKDs, and (c) 3-TMDs and 3-EKDs, against the NC structure.

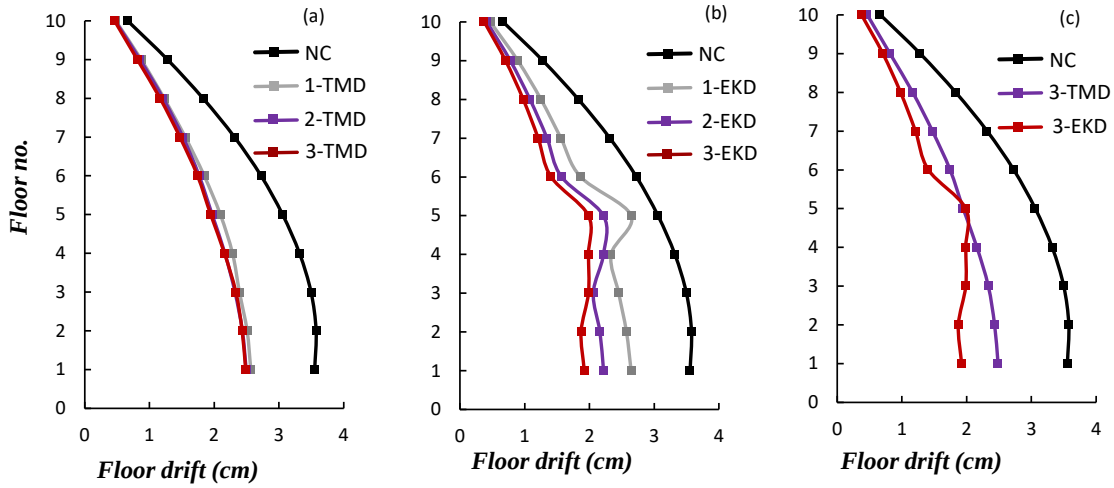

Figure 7. Floor drift envelopes, for the (a) d-TMDs, (b) d-EKDs, and (c) 3-TMDs and 3-EKDs, against the NC structure.

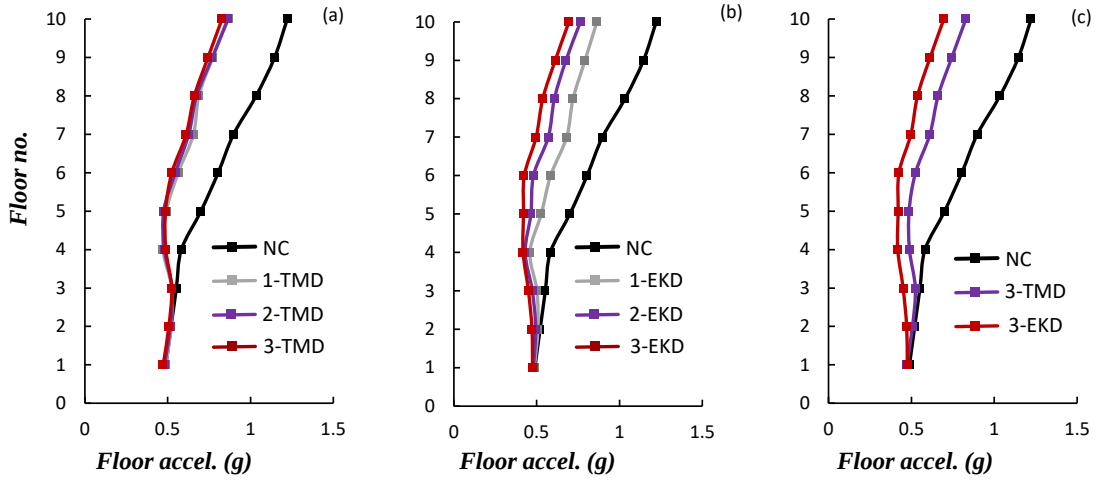

Figure 8. Absolute floor acceleration envelopes, for the (a) d-TMDs, (b) d-EKDs, and (c) 3-TMDs and 3-EKDs, against the NC structure.

5.2 Selection of Real Ground Motions & Performance Criteria

Aiming to validate the efficiency of the d-EKDs proposed methodology and examine the dynamic performance of the system, an ensemble of eight (8) recorded, real earthquake motions is adopted as input seismic excitation to the benchmark structure. The selected records from the US, European and Asian region cover a wide range and variety of key seismic characteristics, such as *PGA*, magnitude (M_w), broad frequency content, duration as well as number of significant acceleration cycles. The characteristics of the selected seismic excitations are provided in Table 3. Time-history analyses are subsequently undertaken for all selected records and a comparison between the performance of the initial/uncontrolled structure, the building with TMDs and the buildings with the d-EKDs is undertaken.

Table 3 Properties of selected real ground records.

No	Earthquake	Year	Station	Ground Motion	Mw	PGA (*g*)	PGA/PGV (*g*×*sec/m*)	R_{jb} (*km*)	$DUR_{5\text{-}75\%}$ (*sec*)
1	Northridge	1994	N Hollywood	Near fault	6.69	0.3087	1.4389	7.89	7.0
2	L'Aquila	2009	V. Aterno	Near fault	6.3	0.4018	1.2548	0.0	4.7
3	Kocaeli	1999	Izmit	Near fault	7.51	0.1651	0.7396	3.62	8.2
4	Tabas	1978	Tabas	Near fault	7.35	0.8540	0.8639	1.79	8.3
5	Kobe	1995	Amagasaki	Near fault	6.9	0.2758	0.8214	11.34	6.9
6	Landers	1992	Joshua tree	Near fault	7.28	0.2736	1.0125	11.03	21.7
7	Duzce	1999	Lamont 1059	Near fault	7.14	0.1524	1.1844	4.17	10.4
8	Friuli	1976	Tolmezzo	Near fault	6.5	0.3571	1.5629	14.97	2.5

The behavior of the benchmark building is assessed based on a set of dynamic response performance criteria (PC_i), evaluated for the previously mentioned real earthquake records. The first criterion (PC_1) is a non-dimensionalized measure of the structure floor displacement relative to the ground, which is provided by:

$$PC_1 = \max\left\{\frac{\max\left|X_i(t)\right|}{X_{NC}^{\max}}\right\}, \quad i=1:N, \quad N=10 \tag{29}$$

where $\left|X_i(t)\right|$ is the absolute i^{th} floor displacement value of the time-history response of the structure with the DVAs, and $X_{NC}^{\max}$ is the maximum displacement of any floor of the NC building. The second performance criterion (PC_2) is the maximum floor drift ratio. The drift ratios are non-dimensionalized by normalizing with respect to the associated floor height of each storey. Thus, the PC_2 performance criterion is given by:

$$PC_2 = \max\left\{\frac{\max\left|d_i(t)\right|/h_i}{d_{NC}^{\max}}\right\}, \quad i=1:N, \quad N=10 \tag{30}$$

where $\left|d_i(t)\right|$ is the absolute value of the inter-storey drift of the i^{th} floor with the DVAs, h_i is the height of the associated storey, and $d_{NC}^{\max}$ is the maximum inter-storey drift ratio of the uncontrolled NC structure. The third performance criterion (PC_3) is the maximum absolute floor acceleration, which is given by:

$$PC_3 = \max\left\{\frac{\max\left|\ddot{X}_i(t)\right|}{\ddot{X}_{NC}^{\max}}\right\}, \quad i=1:N, \quad N=10 \tag{31}$$

where $\left|\ddot{X}_i(t)\right|$ is the absolute maximum value of the time history i^{th} floor absolute acceleration, and $\ddot{X}_{NC}^{\max}$ is the maximum value of the absolute floor acceleration of the NC building. The fourth and final performance criterion (PC_4) related to the structural dynamic response is the maximum non-dimensionalized base shear:

$$PC_4 = \max\left\{\frac{\max\left|\sum_{1}^{N+n} M_i\ddot{X}_i(t)\right|}{VB_{NC}^{\max}}\right\}, \quad i=1:(N+n), \quad N=10, \quad n=3 \tag{32}$$

where $VB_{NC}^{\max}$ is the maximum base shear of the NC structure, and M_i is the seismic mass of the i^{th} floor. To assess the performance of the distributed EKD devices, two additional performance criteria are formed. The first one (PC_5) is the negative stiffness (NS) stroke $X_{NS\text{-}i}$, which is defined as the relative displacement between the terminals of the $k_{N\text{-}i}$ and is critical for the realistic design of the configuration that generates controlled NS, given by:

$$PC_5 = \max\left\{\frac{\max\left|X_{NS-i}(t)\right|}{X_{NS}^{\lim}}\right\}, \quad i=1:n, \quad n=3 \tag{33}$$

where $X_{NS\text{-}i}$ is the NS stroke of the EKD number (i). The second performance criterion (PC_6) of the EKD device is the relative to the ground displacement of the additional

oscillating mass of the controller device, which is given by:

$$PC_6 = \max\left\{\frac{\max\left|X_{EKD-i}(t)\right|}{X_{NC}^{\max}}\right\}, \quad i = 1{:}10 \tag{34}$$

5.3 Performance Assessment of the d-EKDs Against Real Seismic Records

In this section, an assessment of the response of the d-EKDs against the 8 selected real seismic records is undertaken and results are provided for a set of performance criteria, described in the previous section of this paper. A comparison of the system with the d-EKD upgrade mechanism against the d-TMDs, as well as the uncontrolled structure is provided herein and results showcase the beneficial vibration control properties of the proposed mechanism.

Specifically, in Figs. 9-12 a plot of each performance criterion (PC1 to PC4) versus the number of employed devices is provided for all earthquake records and for both upgrade frameworks (d-TMDs and d-EKDs). Results show that the proposed mechanism presents superior (or similar) vibration control properties compared to the d-TMD system, for all seismic cases. This is a clear indication that the d-EKDs may act as an enhanced TMD without the need of heavy additional masses (the d-EKDs obtain only 10% of the d-TMDs total mass). In addition, it appears that the installation of more than 1-TMD devices does not significantly alter the dynamic response of the structure. This is attributed to the fact that for this mid-rise structure the fundamental eigenfrequency of the building affects significantly the dynamic response of the structure and hence, seeking to mitigate vibration due to the remaining eigenmodes is not substantially effective. However, as clearly observed in the performance criteria results, the d-EKD concept is more effective as the number of EKD devices increases; the EKD is a stiffness-based vibration control device that is not frequency dependent

and provides damping properties to a broad bandwidth (K.A. Kapasakalis, Antoniadis, and Sapountzakis 2020). Consequently, increasing the number of the optimized d-EKDs provides additional damping to the system without the need to alter the eigenfrequencies of the structure.

For the selected performance criteria, we observe the following:

- **For the case of the d-EKDs** total displacements (PC1) are reduced approximately at a range of 10-50%, floor drifts (PC2) are reduced from 10-55%, accelerations (PC3) from 20-55%, and base shear (PC4) is decreased from 10-55%.
- **For the case of the d-TMDs** total displacements (PC1) are reduced approximately at a range of 0-30%, floor drifts (PC2) are reduced from 0-35%, accelerations (PC3) from 10-40%, and base shear (PC4) is decreased from 0-35%.

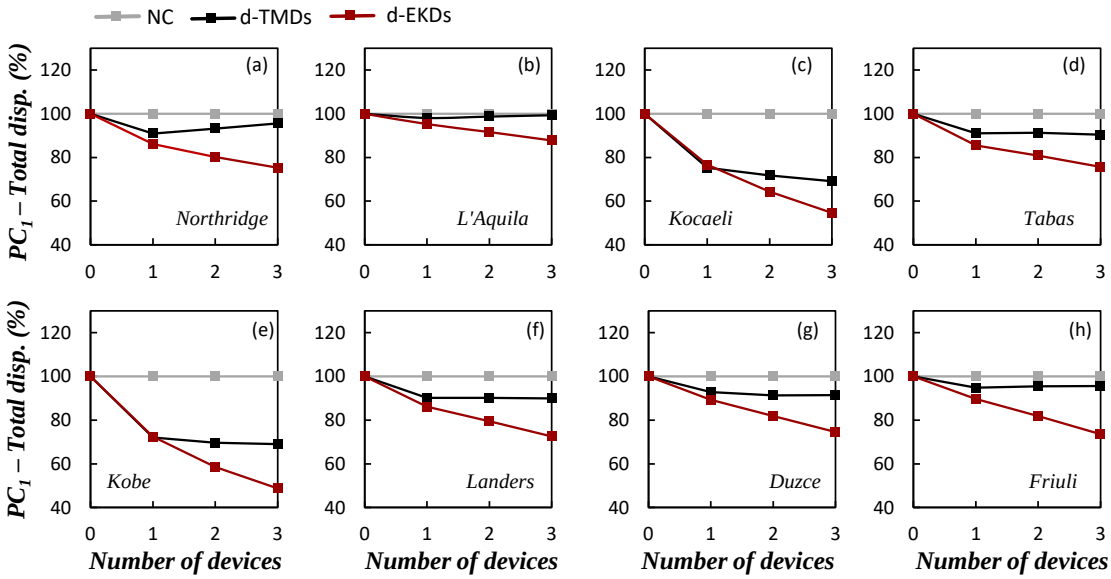

Figure 9. Variation of PC1 – total displacement with respect to the number of installed devices (d-TMDs, d-EKDs) for all the considered real ground motions.

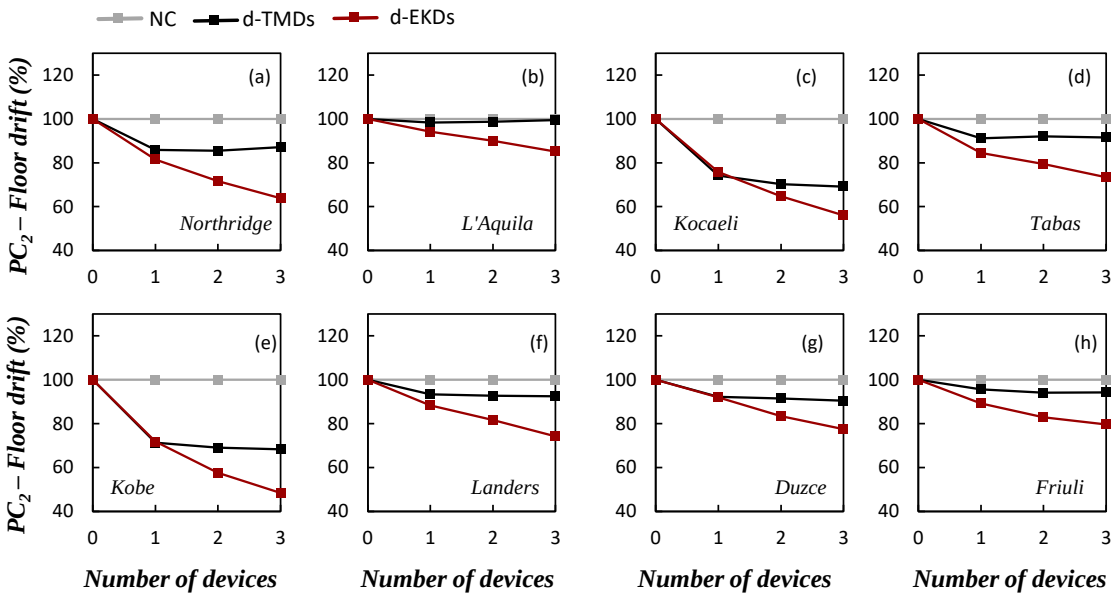

Figure 10. Variation of PC2 – floor drift with respect to the number of installed devices (d-TMDs, d-EKDs) for all the considered real ground motions.

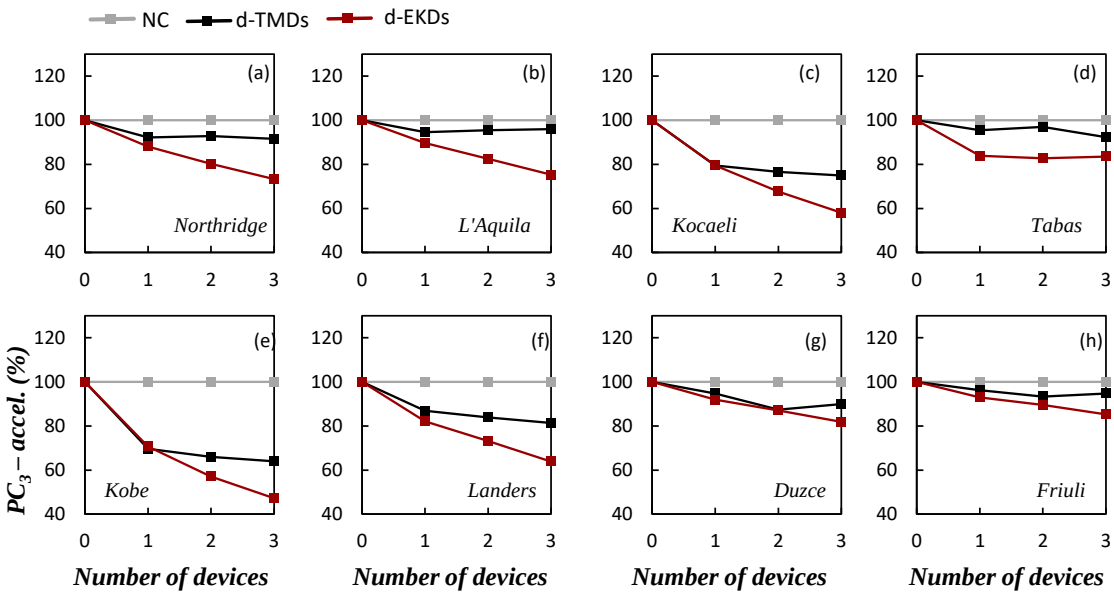

Figure 11. Variation of PC3 – absolute acceleration with respect to the number of installed devices (d-TMDs, d-EKDs) for all the considered real ground motions.

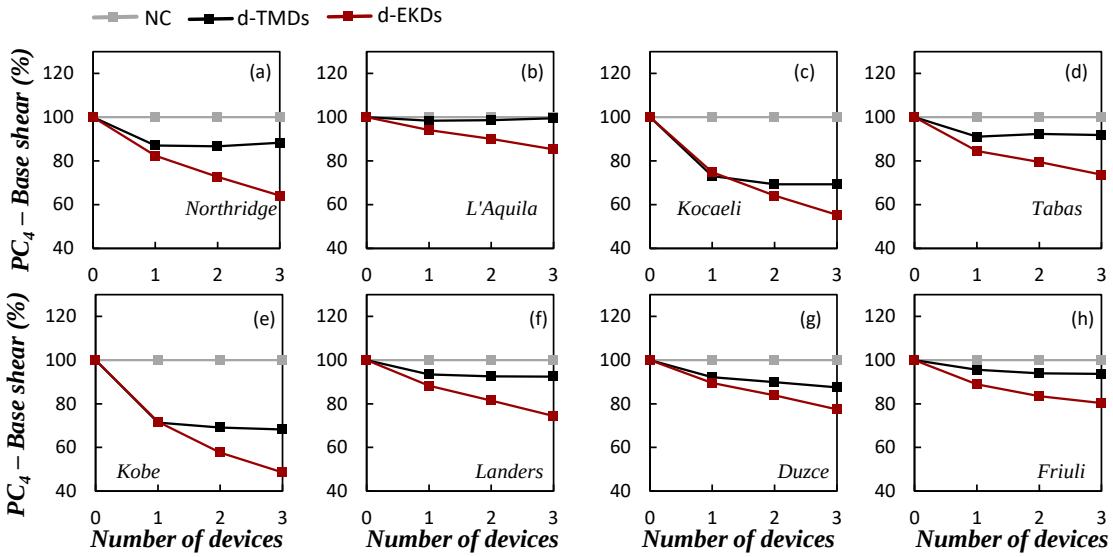

Figure 12. Variation of PC4 – base shear with respect to the number of installed devices (d-TMDs, d-EKDs) for all the considered real ground motions.

A summary of the average reduction of the absolute displacements, drifts, absolute accelerations and base shear for all selected real earthquake records, for the system with the d-EKDs and the d-TMDs respectively, is presented Table 4. Specifically for the 1-EKD, 2-EKDs, and 3-EKD the structural dynamic responses (mean of max values for all the examined real earthquakes) are improved approximately by 15%, 23%, and 30%, while when 1-TMD, 2-TMDs, and 3-TMDs are installed, the respective reductions in the dynamic responses are 12%, 13%, and 14%.

Table 4: Average reduction (based on the performance criteria PC1-4) of total displacements, drifts, absolute accelerations, and base shear for all selected real earthquake records, for the d-EKD and d-TMD systems.

System	Total Displacements Reduction (%), (PC1)	Drifts Reduction (%), (PC2)	Absolute Acceleration Reduction (%), (PC3)	Base Shear Reduction (%), (PC4)
1-EKD	14.9	15.4	15.2	15.7
2-EKDs	22.7	23.6	22.5	23.4
3-EKDs	29.7	30.2	29.0	30.1
1-TMD	11.9	12.2	11.4	12.2
2-TMDs	12.3	13.3	13.5	13.4
3-TMDs	12.5	13.4	14.4	13.7

Fig. 13 illustrates indicative time-history analyses results for the case of Northridge (1994) and Kobe (1995) earthquake records. The plots present a comparison between the uncontrolled structure and the building with 3-TMDs and 3-EKDs respectively. By all means, for both cases the d-EKD system outperforms the traditional d-TMDs, highlighting the efficiency of the system. The dynamic responses of the NC system and the system with the d-TMDs and the d-EKDs can be found in Appendix C.

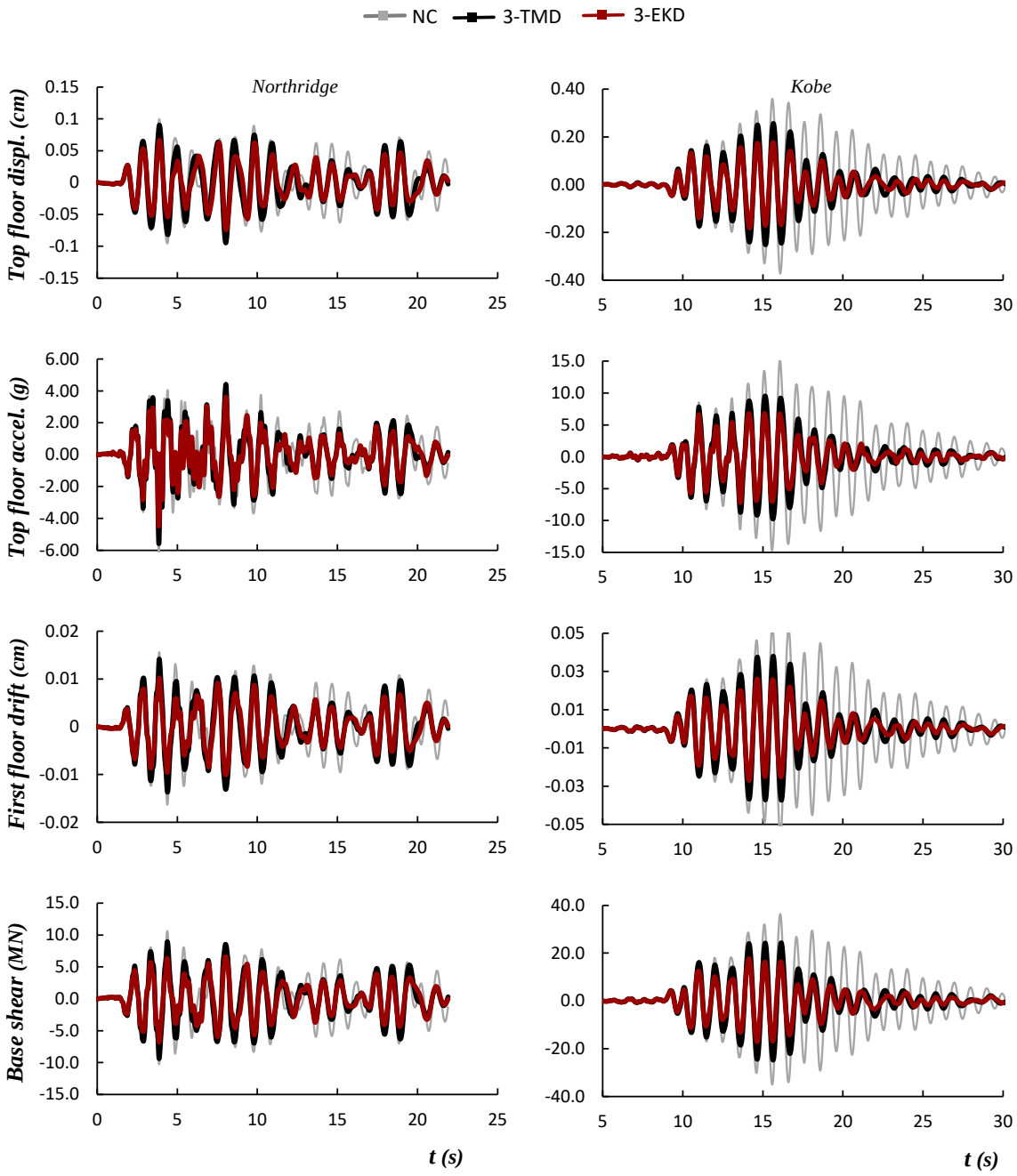

Figure 13. Comparative time history results between the NC system and the system with the d-TMDs and the d-EKDs in terms of top floor displacements, accelerations, first floor drifts, and base shear for the Northridge, and Kobe earthquakes respectively.

6. Conclusions

In this research work, a framework towards the seismic protection of a mid-rise building with distributed extended KDamper (d-EKD) devices is examined. The d-EKD vibration control concept is designed with significantly small additional oscillating masses in order to avoid burdening the structure. In addition, the system parameters are selected following a constrained optimization approach that imposes proper constraints and limitations to the structural dynamic response, as well as in the values of the design variables. In addition, static and dynamic structural stability is ensured with the presented stability conditions. The performance of the controlled structure is assessed with real strong ground motions, and by adopting several performance criteria, commonly used in the literature. A comparison with distributed Tuned Mass Dampers (d-TMDs) is undertaken in order to prove the efficiency of the proposed seismic protection approach. Based on the dynamic analysis and the results obtained, the following major concluding remarks are highlighted:

(1) The design of the d-EKD is realistic, as it foresees variation in the value of the negative stiffness element to ensure stability, assumes minimal additional mass, and imposes limitations to the design variables, rendering the design feasible within reasonable technological capabilities.

(2) The controlled with the d-EKD superstructure's dynamic behavior is superior to that of the d-TMD regardless of the installed devices, introducing significantly smaller additional masses (ten times smaller). More specifically, for the case of 3 implemented devices, the 3-EKDs further reduce the building structure's dynamic responses (mean of max values for all the examined real earthquakes) by more than 15%, as compared to the 3-TMDs.

(3) The d-EKD performance is enhanced by increasing the number of implemented devices, while for the d-TMD approach the mitigation of the dynamic responses is slightly affected. In particular, in the case where the implemented devices are 1-EKD, 2-EKDs, and 3-EKD, the respective reductions (mean of max values for all the examined real earthquakes) in the structural dynamic responses are 15.3%, 23.0%, and 29.7%, while when 1-TMD, 2-TMDs, and 3-TMDs are installed, the respective reductions are 11.9%, 13.1%, and 13.5%.

(4) The d-EKD offers a more broadband response compared to the d-TMD, as its performance is not directly affected by the device tuning frequency but rather by the optimal combination of the stiffness elements, positive and negative.

7. Declarations

Funding Details This work was supported by the European Union's Horizon 2020 research and innovation program under the Marie Sklodowska-Curie grant (Grant Agreement No. INSPIRE-813424, "INSPIRE—Innovative Ground Interface Concepts for Structure Protection").

Acknowledgments Dr. Konstantinos Kapasakalis would like to acknowledge the support by the Bodossaki Foundation – Scholarship for Postdoctoral studies.

Disclosure Statement The authors report there are no competing interests to declare.

Data Availability Statement The data used to support the findings of this study are available from the corresponding author upon request.

8. References

Abé, Masato, and Yozo Fujino. 1994. Dynamic Characterization of Multiple Tuned Mass Dampers and Some Design Formulas. *Earthquake Engineering & Structural Dynamics* 23 (8). John Wiley & Sons, Ltd:813–835. doi:10.1002/EQE.4290230802.

Acar, M. A., and C. Yilmaz. 2013. Design of an Adaptive-Passive Dynamic Vibration Absorber Composed of a String-Mass System Equipped with Negative Stiffness Tension Adjusting Mechanism. *Journal of Sound and Vibration* 332 (2):231–245. doi:10.1016/j.jsv.2012.09.007.

Andreas, Paradeisiotis, Kalderon Moris, Antoniadis Ioannis, and Fouriki Lina. 2020. Acoustic Performance Evaluation of a Panel Utilizing Negative Stiffness Mounting for Low Frequency Noise Control. *Proceedings of the International Conference on Structural Dynamic , EURODYN* 2. European Association for Structural Dynamics:4093–4110. doi:10.47964/1120.9335.19276.

Antoniadis, Ioannis A., Stratis A. Kanarachos, Konstantinos Gryllias, and Ioannis E. Sapountzakis. 2018. KDamping: A Stiffness Based Vibration Absorption Concept. *JVC/Journal of Vibration and Control* 24 (3):588–606. doi:10.1177/1077546316646514.

Ayorinde, E. O., and G. B. Warburton. 1980. Minimizing Structural Vibrations with Absorbers. *Earthquake Engineering & Structural Dynamics* 8 (3). John Wiley & Sons, Ltd:219–236. doi:10.1002/EQE.4290080303.

Bakre, S. V., and R. S. Jangid. 2007. Optimum Parameters of Tuned Mass Damper for Damped Main System. *Structural Control and Health Monitoring* 14 (3). John

Wiley & Sons, Ltd:448–470. doi:10.1002/STC.166.

Bhowmik, Kamalesh, and Nirmalendu Debnath. 2021. On Stochastic Design of Negative Stiffness Integrated Tuned Mass Damper (NS-TMD). *Journal of Vibration Engineering and Technologies* 9 (8). Springer:2197–2211. doi:10.1007/S42417-021-00356-0/FIGURES/13.

Chen, Genda, and Jingning Wu. 2001. Optimal Placement of Multiple Tune Mass Dampers for Seismic Structures. *Journal of Structural Engineering* 127 (9). American Society of Civil Engineers:1054–1062. doi:10.1061/(ASCE)0733-9445(2001)127:9(1054).

Chen, Huating, Kaiming Bi, Yanhui Liu, and Ping Tan. 2022. Performance Evaluation of Multiple Tuned Inerter-Based Dampers for Seismic Induced Structural Vibration Control. *Structural Control and Health Monitoring* 29 (1):e2860. doi:https://doi.org/10.1002/stc.2860.

Cheng, Zhibao, Antonio Palermo, Zhifei Shi, and Alessandro Marzani. 2020. Enhanced Tuned Mass Damper Using an Inertial Amplification Mechanism. *Journal of Sound and Vibration* 475 (June). Academic Press:115267. doi:10.1016/J.JSV.2020.115267.

Chowdhury, S., A. Banerjee, and S. Adhikari. 2022. Optimal Negative Stiffness Inertial-Amplifier-Base-Isolators: Exact Closed-Form Expressions. *International Journal of Mechanical Sciences* 218 (March). Pergamon:107044. doi:10.1016/J.IJMECSCI.2021.107044.

Clark, a. J. 1988. Multiple Passive Tuned Mass Damper for Reducing Earthquake Induced Building Motion. *9th World Conference in Earthquake Engineering*.

Dadkhah, Masoud, Reza Kamgar, Heisam Heidarzadeh, Anna Jakubczyk-Galczyńska, and Robert Jankowski. 2020. Improvement of Performance Level of Steel Moment-Resisting Frames Using Tuned Mass Damper System. *Applied Sciences 2020, Vol. 10, Page 3403* 10 (10). Multidisciplinary Digital Publishing Institute:3403. doi:10.3390/APP10103403.

De Domenico, Dario, and Giuseppe Ricciardi. 2018. Earthquake-Resilient Design of Base Isolated Buildings with TMD at Basement: Application to a Case Study. *Soil Dynamics and Earthquake Engineering* 113 (October). Elsevier Ltd:503–521. doi:10.1016/j.soildyn.2018.06.022.

Den Hartog, J P. 1956. *Mechanical Vibrations*. *McGraw-Hill, New York*. 4th ed. New York. doi:10.1038/161503c0.

Elias, Said, and Vasant Matsagar. 2015. Optimum Tuned Mass Damper for Wind and Earthquake Response Control of High-Rise Building. *Advances in Structural Engineering: Dynamics, Volume Two*, 751–1616. doi:10.1007/978-81-322-2193-7.

Elias, Said, Vasant Matsagar, and T. K. Datta. 2016. Effectiveness of Distributed Tuned Mass Dampers for Multi-Mode Control of Chimney under Earthquakes. *Engineering Structures* 124. Elsevier Ltd:1–16. doi:10.1016/j.engstruct.2016.06.006.

Elias, Said, Vasant Matsagar, and T. K. Datta. 2017. Distributed Tuned Mass Dampers for Multi-Mode Control of Benchmark Building under Seismic Excitations. *Https://Doi.Org/10.1080/13632469.2017.1351407* 23 (7). Taylor & Francis:1137–1172. doi:10.1080/13632469.2017.1351407.

Emami, Fereshteh, and Milad Tayefeh Mohammad Ali. 2022. Evaluation of Seismic

Response of the Straight Concrete Bridges with Three Methods of Passive Control (K-Damper, TMD and LRB). *Journal of Structural and Construction Engineering* 8 (Special Issue 4). Iranian Society of Structural Engineering (ISSE):46–60. doi:10.22065/JSCE.2021.228042.2129.

Etedali, Sadegh, and Hojjat Rakhshani. 2018. Optimum Design of Tuned Mass Dampers Using Multi-Objective Cuckoo Search for Buildings under Seismic Excitations. *Alexandria Engineering Journal* 57 (4). Elsevier:3205–3218. doi:10.1016/J.AEJ.2018.01.009.

Fahim, Sadek;, Mohraz; Bijan, Taylor; Andrew, and Chung; Riley. 1998. A METHOD OF ESTIMATING THE PARAMETERS OF TUNED MASS DAMPERS FOR SEISMIC APPLICATIONS. *Earthq. Eng. Struct. Dyn* 26 (6):617–635. doi:https://doi.org/10.1002/(SICI)1096-9845(199706)26:6<617::AID-EQE664>3.0.CO;2-Z.

Farag, Mousa M.N., Sameh S.F. Mehanny, and Mourad M. Bakhoum. 2015. Establishing Optimal Gap Size for Precast Beam Bridges with a Buffer-Gap-Elastomeric Bearings System. *Earthquake and Structures* 9 (1):195–219. doi:10.12989/eas.2015.9.1.195.

Frahm, H. 1911. Device for Damping of Bodies. *U.S. Patent*.

Giaralis, A., and A. A. Taflanidis. 2018. Optimal Tuned Mass-Damper-Inerter (TMDI) Design for Seismically Excited MDOF Structures with Model Uncertainties Based on Reliability Criteria. *Structural Control and Health Monitoring*. doi:10.1002/stc.2082.

Hadi, Muhammad N. S., and Yoyong Arfiadi. 1998. Optimum Design of Absorber for

MDOF Structures. *Journal of Structural Engineering* 124 (11). American Society of Civil Engineers:1272–1280. doi:10.1061/(ASCE)0733-9445(1998)124:11(1272).

Hoang, Nam, Yozo Fujino, and Pennung Warnitchai. 2008. Optimal Tuned Mass Damper for Seismic Applications and Practical Design Formulas. *Engineering Structures* 30 (3). Elsevier:707–715. doi:10.1016/J.ENGSTRUCT.2007.05.007.

Igusa, T., and K. Xu. 1994. Vibration Control Using Multiple Tuned Mass Dampers. *Journal of Sound and Vibration* 175 (4). Academic Press:491–503. doi:10.1006/JSVI.1994.1341.

Jangid, R. S. 2021. Optimum Tuned Inerter Damper for Base-Isolated Structures. *Journal of Vibration Engineering and Technologies* 9 (7). Springer:1483–1497. doi:10.1007/S42417-021-00309-7/FIGURES/12.

Jiang, Shaodong, Kaiming Bi, Ruisheng Ma, Qiang Han, and Xiuli Du. 2023. Influence of Spatially Varying Ground Motions on the Seismic Responses of Bridge Structures with KDampers. *Engineering Structures* 277 (February). Elsevier:115461. doi:10.1016/J.ENGSTRUCT.2022.115461.

Kalderon, Moris, Antonios Mantakas, Andreas Paradeisiotis, Ioannis Antoniadis, and Evangelos J. Sapountzakis. 2022. Locally Resonant Metamaterials Utilizing Dynamic Directional Amplification: An Application for Seismic Mitigation. *Applied Mathematical Modelling* 110 (October). Elsevier:1–16. doi:10.1016/J.APM.2022.05.037.

Kalderon, Moris, Antonis Mantakas, and Ioannis Antoniadis. 2023. Dynamic Modelling and Experimental Testing of a Dynamic Directional Amplification Mechanism for

Vibration Mitigation. *Journal of Vibration Engineering & Technologies*. doi:10.1007/s42417-023-00925-5.

Kalderon, Moris, Andreas Paradeisiotis, and Ioannis Antoniadis. 2021. A Meta-Structure for Low-Frequency Acoustic Treatment Based on a KDamper-Inertial Amplification Concept. In *Euronoise 2021*, 1333–1343.

Kalogerakou, M., A. Paradeisiotis, and I. Antoniadis. 2023. Vertical Seismic Absorber Utilizing Inertance and Negative Stiffness Implemented with Gas Springs. *Earthquake Engineering and Engineering Vibration*, January. Institute of Engineering Mechanics (IEM), 1–17. doi:10.1007/S11803-023-2163-2/METRICS.

Kalogerakou, Marina E., Konstantinos A. Kapasakalis, Ioannis A. Antoniadis, and Evangelos J. Sapountzakis. 2023. Vertical Seismic Protection of Structures with Inerter-Based Negative Stiffness Absorbers. *Bulletin of Earthquake Engineering* 21 (3):1439–1480. doi:10.1007/s10518-021-01284-w.

Kamgar, R., H. Heidarzadeh, and M. R. Babadaei Samani. 2021. Evaluation of Buckling Load and Dynamic Performance of Steel Shear Wall Retrofitted with Strips Made of Shape Memory Alloy. *Scientia Iranica* 28 (3). Sharif University of Technology:1096–1108. doi:10.24200/SCI.2020.52994.2991.

Kamgar, Reza, Fatemeh Gholami, Hamed Reza Zarif Sanayei, and Heisam Heidarzadeh. 2020. Modified Tuned Liquid Dampers for Seismic Protection of Buildings Considering Soil–Structure Interaction Effects. *Iranian Journal of Science and Technology - Transactions of Civil Engineering* 44 (1). Springer:339–354. doi:10.1007/S40996-019-00302-X/TABLES/5.

Kamgar, Reza, and Mohammad Reza Babadaei Samani. 2021. Numerical Study for

Evaluating the Effect of Length-to-Height Ratio on the Behavior of Concrete Frame Retrofitted with Steel Infill Plates. *Practice Periodical on Structural Design and Construction* 27 (1). American Society of Civil Engineers:04021062. doi:10.1061/(ASCE)SC.1943-5576.0000632.

Kamgar, Reza, Parham Samea, and Mohsen Khatibinia. 2018. Optimizing Parameters of Tuned Mass Damper Subjected to Critical Earthquake. *The Structural Design of Tall and Special Buildings* 27 (7). John Wiley & Sons, Ltd:e1460. doi:10.1002/TAL.1460.

Kampitsis, Andreas, Konstantinos Kapasakalis, and Lluis Via-Estrem. 2022. An Integrated FEA-CFD Simulation of Offshore Wind Turbines with Vibration Control Systems. *Engineering Structures* 254 (March). Elsevier:113859. doi:10.1016/J.ENGSTRUCT.2022.113859.

Kapasakalis, K.A., I.A. Antoniadis, and E.J. Sapountzakis. 2020. Performance Assessment of the KDamper as a Seismic Absorption Base. *Structural Control and Health Monitoring* 27 (4). doi:10.1002/stc.2482.

Kapasakalis, K.A., I.A. Antoniadis, and E.J. Sapountzakis. 2021. Constrained Optimal Design of Seismic Base Absorbers Based on an Extended KDamper Concept. *Engineering Structures* 226. doi:10.1016/j.engstruct.2020.111312.

Kapasakalis, KA, IA Antoniadis, and EJ Sapountzakis. 2019. Implementation of the KDamper Concept for Base Isolation to a Typical Concrete Building Structure. In *Proceedings of the 12th International Congress on Mechanics (12HSTAM2019)*.

Kapasakalis, Konstantinos A., Ioannis A. Antoniadis, and Evangelos J. Sapountzakis. 2021a. STIFF Vertical Seismic Absorbers. *JVC/Journal of Vibration and Control* 0

(0). SAGE Publications Inc.:1–13. doi:10.1177/10775463211001624.

Kapasakalis, Konstantinos A., Ioannis A. Antoniadis, and Evangelos J. Sapountzakis. 2021b. Feasibility Assessment of Stiff Seismic Base Absorbers. *Journal of Vibration Engineering & Technologies 2021*, August. Springer, 1–17. doi:10.1007/S42417-021-00362-2.

Kapasakalis, Konstantinos A., Ioannis A. Antoniadis, and Evangelos J. Sapountzakis. 2022. STIFF Vertical Seismic Absorbers. *JVC/Journal of Vibration and Control* 28 (15–16). SAGE Publications Inc.:1937–1949. doi:10.1177/10775463211001624/ASSET/IMAGES/LARGE/10.1177_10775463211001624-FIG2.JPEG.

Kareem, Ahsan. 1983. Mitigation of Wind Induced Motion of Tall Buildings. *Journal of Wind Engineering and Industrial Aerodynamics* 11 (1–3):273–284. doi:10.1016/0167-6105(83)90106-X.

Kareem, Ahsan, Tracy Kijewski, and Yukio Tamura. 1999. Mitigation of Motions of Tall Buildings with Specific Examples of Recent Applications. *Wind and Structures, An International Journal* 2 (3). Techno- Press:201–251. doi:10.12989/WAS.1999.2.3.201.

Kareem, Ahsan, and Samuel Kline. 1995. Performance of Multiple Mass Dampers under Random Loading. *Journal of Structural Engineering* 121 (2). American Society of Civil Engineers:348–361. doi:10.1061/(ASCE)0733-9445(1995)121:2(348).

Kelly, James M. 1999. The Role of Damping in Seismic Isolation. *Earthquake Engineering and Structural Dynamics* 28 (1):3–20. doi:10.1002/(SICI)1096-

9845(199901)28:1<3::AID-EQE801>3.0.CO;2-D.

Khatibinia, Mohsen, Hossein Gholami, and Reza Kamgar. 2018. Optimal Design of Tuned Mass Dampers Subjected to Continuous Stationary Critical Excitation. *International Journal of Dynamics and Control* 6 (3). Springer Berlin Heidelberg:1094–1104. doi:10.1007/S40435-017-0386-7/FIGURES/10.

Li, Chunxiang. 2002. Optimum Multiple Tuned Mass Dampers for Structures under the Ground Acceleration Based on DDMF and ADMF. *Earthquake Engineering & Structural Dynamics* 31 (4). John Wiley & Sons, Ltd:897–919. doi:10.1002/EQE.128.

Li, Huan, Yancheng Li, and Jianchun Li. 2020. *Negative Stiffness Devices for Vibration Isolation Applications: A Review*. *Advances in Structural Engineering*. Vol. 23. SAGE Publications Inc. doi:10.1177/1369433219900311.

Mane, Pravin Uttam, and Gangadhar Ramrao Kondekar. 2021. Experimental Study on Vibration Control Using Shape Memory Alloy Based Vibration Absorber. *Materials Today: Proceedings* 45 (January). Elsevier:2812–2817. doi:10.1016/J.MATPR.2020.11.802.

Mantakas, Antonios G., Konstantinos A. Kapasakalis, Antonios E. Alvertos, Ioannis A. Antoniadis, and Evangelos J. Sapountzakis. 2022. A Negative Stiffness Dynamic Base Absorber for Seismic Retrofitting of Residential Buildings. *Structural Control and Health Monitoring*. John Wiley & Sons, Ltd, e3127. doi:10.1002/STC.3127.

Marian, Laurentiu, and Agathoklis Giaralis. 2014. Optimal Design of a Novel Tuned Mass-Damper-Inerter (TMDI) Passive Vibration Control Configuration for

Stochastically Support-Excited Structural Systems. *Probabilistic Engineering Mechanics* 38. Elsevier:156–164. doi:10.1016/j.probengmech.2014.03.007.

Naeim, Farzad., and James M. Kelly. 1999. *Design of Seismic Isolated Structures : From Theory to Practice*. John Wiley. https://www.wiley.com/en-us/Design+of+Seismic+Isolated+Structures%3A+From+Theory+to+Practice-p-9780471149217.

Naeim, Farzad. 1998. Performance of 20 Extensively-Instrumented Buildings during the 1994 Northridge Earthquake. *The Structural Design of Tall Buildings* 7 (3). Wiley Online Library:179–194.

Nagarajaiah, Satish, and Ertan Sonmez. 2007. Structures with Semiactive Variable Stiffness Single/Multiple Tuned Mass Dampers. *Journal of Structural Engineering* 133 (1):67–77. doi:10.1061/(asce)0733-9445(2007)133:1(67).

Paradeisiotis, Andreas, Moris Kalderon, and Ioannis Antoniadis. 2021. Advanced Negative Stiffness Absorber for Low-Frequency Noise Insulation of Panels. *AIP Advances* 11 (6). AIP Publishing LLCAIP Publishing:065003. doi:10.1063/5.0045937.

Radmard Rahmani, Hamid, and Carsten Könke. 2019. Seismic Control of Tall Buildings Using Distributed Multiple Tuned Mass Dampers. *Advances in Civil Engineering* 2019. doi:10.1155/2019/6480384.

Salimi, Mitra, Reza Kamgar, and Heisam Heidarzadeh. 2021. An Evaluation of the Advantages of Friction TMD over Conventional TMD. *Innovative Infrastructure Solutions* 6 (2). Springer Science and Business Media Deutschland GmbH:1–12. doi:10.1007/S41062-021-00473-5/FIGURES/7.

Singh, M. P., E. E. Matheu, and L. E. Suarez. 1998. ACTIVE AND SEMI-ACTIVE CONTROL OF STRUCTURES UNDER SEISMIC EXCITATION. *Earthquake Engineering & Structural Dynamics* 26 (2):193–213. doi:https://doi.org/10.1002/(SICI)1096-9845(199702)26:2<193::AID-EQE634>3.0.CO;2-%23.

Sladek, John R., and Richard E. Klingner. 1983. Effect of TunedMass Dampers on Seismic Response. *Journal of Structural Engineering* 109 (8). American Society of Civil Engineers:2004–2009. doi:10.1061/(ASCE)0733-9445(1983)109:8(2004).

Smith, Malcolm C. 2002. Synthesis of Mechanical Networks: The Inerter. *IEEE TRANSACTIONS ON AUTOMATIC CONTROL* 47 (10). doi:10.1109/TAC.2002.803532.

Suresh, Lekshmi, and K. M. Mini. 2019. Effect of Multiple Tuned Mass Dampers for Vibration Control in High-Rise Buildings. *Practice Periodical on Structural Design and Construction* 24 (4):1–13. doi:10.1061/(asce)sc.1943-5576.0000453.

Symans, M. D., F. A. Charney, A. S. Whittaker, M. C. Constantinou, C. A. Kircher, M. W. Johnson, and R. J. McNamara. 2007. Energy Dissipation Systems for Seismic Applications: Current Practice and Recent Developments. *Journal of Structural Engineering* 134 (1):3–21. doi:10.1061/(asce)0733-9445(2008)134:1(3).

Syrimi, Panagiota, Evangelos Sapountzakis, George Tsiatas, and Ioannis Antoniadis. 2017. Parameter Optimization of the Kdamper Concept in Seismic Isolation of Bridges Using Harmony Search Algorithm. In *In: Proc of the 6th COMPDYN 2017, Rhodes Island, Greece*, 37–51. doi:10.7712/120117.5408.17764.

Taniguchi, Tomoyo, Armen Der Kiureghian, and Mikayel Melkumyan. 2008. Effect of

Tuned Mass Damper on Displacement Demand of Base-Isolated Structures. *Engineering Structures* 30 (12):3478–3488. doi:10.1016/j.engstruct.2008.05.027.

Warburton, G. B. 1982. Optimum Absorber Parameters for Various Combinations of Response and Excitation Parameters. *Earthquake Engineering & Structural Dynamics* 10 (3). John Wiley & Sons, Ltd:381–401. doi:10.1002/EQE.4290100304.

Warn, Gordon P., and Keri L. Ryan. 2012. A Review of Seismic Isolation for Buildings: Historical Development and Research Needs. *Buildings* 2 (3):300–325. doi:10.3390/buildings2030300.

Weber, Benedikt, and Glauco Feltrin. 2010. Assessment of Long-Term Behavior of Tuned Mass Dampers by System Identification. *Engineering Structures* 32 (11):3670–3682. doi:10.1016/j.engstruct.2010.08.011.

Xiang, Ping, and Akira Nishitani. 2013. Seismic Vibration Control of Building Structures with Multiple Tuned Mass Damper Fl Oors Integrated. doi:10.1002/eqe.

Xiang, Ping, and Akira Nishitani. 2014. Optimum Design for More Effective Tuned Mass Damper System and Its Application to Base-Isolated Buildings. *Structural Control and Health Monitoring* 21 (1):98–114. doi:10.1002/stc.1556.

Xu, Kangming, and Takeru Igusa. 1992. Dynamic Characteristics of Multiple Substructures with Closely Spaced Frequencies. *Earthquake Engineering & Structural Dynamics* 21 (12):1059–1070. doi:10.1002/eqe.4290211203.

Yamaguchi, Hiroki, and Napat Harnpornchai. 1993. Fundamental Characteristics of Multiple Tuned Mass Dampers for Suppressing Harmonically Forced Oscillations.

Earthquake Engineering & Structural Dynamics 22 (1):51–62. doi:10.1002/eqe.4290220105.

Zong Woo Geem, Joong Hoon Kim, and G.V. Loganathan. 2001. A New Heuristic Optimization Algorithm: Harmony Search. *SIMULATION* 76 (2). Sage PublicationsSage CA: Thousand Oaks, CA:60–68. doi:10.1177/003754970107600201.

Zuo, Haoran, Kaiming Bi, and Hong Hao. 2017. Using Multiple Tuned Mass Dampers to Control Offshore Wind Turbine Vibrations under Multiple Hazards. *Engineering Structures* 141 (June). Elsevier:303–315. doi:10.1016/J.ENGSTRUCT.2017.03.006.

9. Appendix A: Shear building structure

The matrices that are related to the NC shear building structure, modelled as a lumped mass system are defined as follows:

$$\left[M_{STR}\right]=\begin{bmatrix} M_1 & 0 & 0 & \cdots & 0 & 0 & 0 & \cdots & 0 & 0 \\ 0 & M_2 & 0 & \cdots & 0 & 0 & 0 & \cdots & 0 & 0 \\ 0 & 0 & M_3 & \cdots & 0 & 0 & 0 & \cdots & 0 & 0 \\ \vdots & \vdots & \vdots & \ddots & \vdots & \vdots & \vdots & \ddots & \vdots & \vdots \\ 0 & 0 & 0 & \cdots & M_{i-1} & 0 & 0 & \cdots & 0 & 0 \\ 0 & 0 & 0 & \cdots & 0 & M_i & 0 & \cdots & 0 & 0 \\ 0 & 0 & 0 & \cdots & 0 & 0 & M_{i+1} & \cdots & 0 & 0 \\ \vdots & \vdots & \vdots & \ddots & \vdots & \vdots & \vdots & \ddots & \vdots & \vdots \\ 0 & 0 & 0 & \cdots & 0 & 0 & 0 & \cdots & M_{N-1} & 0 \\ 0 & 0 & 0 & \cdots & 0 & 0 & 0 & \cdots & 0 & M_N \end{bmatrix} \quad (35.a)$$

$$[K_{STR}] = \begin{bmatrix} k_1+k_2 & -k_2 & 0 & \cdots & 0 & 0 & 0 & \cdots & 0 & 0 \\ -k_2 & k_2+k_3 & -k_3 & \cdots & 0 & 0 & 0 & \cdots & 0 & 0 \\ 0 & -k_3 & k_3+k_4 & \cdots & 0 & 0 & 0 & \cdots & 0 & 0 \\ \vdots & \vdots & \vdots & \ddots & \vdots & \vdots & \vdots & \ddots & \vdots & \vdots \\ 0 & 0 & 0 & \cdots & k_{i-1}+k_i & -k_i & 0 & \cdots & 0 & 0 \\ 0 & 0 & 0 & \cdots & -k_i & k_i+k_{i+1} & -k_{i+1} & \cdots & 0 & 0 \\ 0 & 0 & 0 & \cdots & 0 & -k_{i+1} & k_{i+1}+k_{i+2} & \cdots & 0 & 0 \\ \vdots & \vdots & \vdots & \ddots & \vdots & \vdots & \vdots & \ddots & \vdots & \vdots \\ 0 & 0 & 0 & \cdots & 0 & 0 & 0 & \cdots & k_{N-1}+k_N & -k_N \\ 0 & 0 & 0 & \cdots & 0 & 0 & 0 & \cdots & -k_N & k_N \end{bmatrix} \quad (35.b)$$

The earthquake ground acceleration is represented by the scalar $\ddot{X}_G$ and $\{r\}$ is the vector of influence coefficients and is defined as $\{r\}_{(N+n)\times 1} = [1, \quad 1, \quad ..., \quad 1]^T$. The dynamic responses of the controlled building structure floor relative to the ground displacement, velocity, and acceleration vectors, as well as the respective dynamic responses of the installed DVAs oscillating masses can be expressed as follows:

$$\{X\} = \{x_{STR-1}, \quad x_{STR-2}, \quad ..., \quad x_{STR-N}, \quad x_{DVA-1}, \quad x_{DVA-2}, \quad ..., \quad x_{DVA-n}\}^T \quad (36.a)$$

$$\{\dot{X}\} = \{\dot{x}_{STR-1}, \quad \dot{x}_{STR-2}, \quad ..., \quad \dot{x}_{STR-N}, \quad \dot{x}_{DVA-1}, \quad \dot{x}_{DVA-2}, \quad ..., \quad \dot{x}_{DVA-n}\}^T \quad (36.b)$$

$$\{\ddot{X}\} = \{\ddot{x}_{STR-1}, \quad \ddot{x}_{STR-2}, \quad ..., \quad \ddot{x}_{STR-N}, \quad \ddot{x}_{DVA-1}, \quad \ddot{x}_{DVA-2}, \quad ..., \quad \ddot{x}_{DVA-n}\}^T \quad (36.c)$$

10. Appendix B: Distributed TMDs (d-TMD)

For each TMD number (i) installed on a floor (j), (Figure 2) the added mass of the TMD is attached to the floor (j) with a positive stiffness element $k_{D\text{-}i}$ and an artificial damper $c_{D\text{-}i}$. The property matrices that account for such an TMD can be formed as follows:

$$K_{DVA}\left(N+i, N+i\right) = k_{D-i} \tag{37.a}$$

$$K_{DVA}\left(N+i, j\right) = -k_{D-i} \tag{37.b}$$

$$K_{DVA}\left(j, N+i\right) = -k_{D-i} \tag{37.c}$$

$$K_{DVA}\left(j, j\right) = k_{D-i} \tag{37.d}$$

$$M_{DVA}\left(N+i, N+i\right) = \mu_i M_{TOT} \tag{38}$$

$$\mu_i = \frac{M_{D-i}}{M_{TOT}} \tag{39.a}$$

$$\mu = \sum_{1}^{n} \mu_i \tag{39.b}$$

$$C_{DVA}\left(N+i, N+i\right) = c_{D-i} \tag{40.a}$$

$$C_{DVA}\left(N+i, j\right) = -c_{D-i} \tag{40.b}$$

$$C_{DVA}\left(j, N+i\right) = -c_{D-i} \tag{40.c}$$

$$C_{DVA}\left(j, j\right) = c_{D-i} \tag{40.d}$$

where μ_i and μ are defined similarly to the d-EKD design as the μ_i is the mass ratio (Eq. (39a) of each TMD number (i), expressed as a percentage of the total superstructure mass M_{TOT}, and μ is the total mass ratio of all the installed TMDs, defined in Eq. (7.b).

11. Appendix C: Dynamic responses of the NC system and the system with the d-TMDs and the d-EKDs

Table 5 Top floor relative to the ground displacement (cm).

Earthquake	NC	1-TMD	1-EKD	2-TMD	2-EKD	3-TMD	3-EKD
Northridge	9.90	9.00	8.53	9.23	7.95	9.46	7.45
L'Aquila	11.16	10.94	10.63	11.01	10.22	11.08	9.79
Kocaeli	11.80	8.88	9.05	8.46	7.59	8.15	6.44
Tabas	26.81	24.41	22.90	24.47	21.65	24.24	20.28
Kobe	37.16	26.78	26.90	25.91	21.78	25.64	18.11
Landers	14.47	13.04	12.47	13.05	11.50	13.01	10.50
Duzce	3.37	3.13	3.01	3.08	2.76	3.08	2.51
Friuli	8.44	8.01	7.57	8.06	6.91	8.07	6.21

Table 6 First floor drift (cm).

Earthquake	NC	1-TMD	1-EKD	2-TMD	2-EKD	3-TMD	3-EKD
Northridge	1.63	1.40	1.33	1.39	1.17	1.42	1.04
L'Aquila	1.74	1.71	1.64	1.72	1.57	1.73	1.48
Kocaeli	1.72	1.27	1.30	1.20	1.11	1.19	0.96
Tabas	3.93	3.58	3.32	3.62	3.12	3.60	2.88
Kobe	5.58	3.98	4.00	3.85	3.21	3.81	2.70
Landers	2.09	1.95	1.84	1.93	1.70	1.93	1.55
Duzce	0.45	0.41	0.41	0.41	0.37	0.40	0.35
Friuli	1.34	1.28	1.19	1.26	1.11	1.26	1.07

Table 7 Top floor absolute acceleration (g).

Earthquake	NC	1-TMD	1-EKD	2-TMD	2-EKD	3-TMD	3-EKD
Northridge	0.62	0.57	0.55	0.58	0.50	0.57	0.46
L'Aquila	0.59	0.56	0.53	0.56	0.49	0.57	0.45
Kocaeli	0.55	0.44	0.44	0.42	0.37	0.41	0.32
Tabas	1.33	1.27	1.11	1.29	1.10	1.22	1.11
Kobe	1.56	1.08	1.10	1.03	0.89	1.00	0.73
Landers	0.63	0.55	0.52	0.53	0.46	0.52	0.40
Duzce	0.22	0.21	0.20	0.19	0.19	0.20	0.18
Friuli	0.53	0.51	0.49	0.49	0.47	0.50	0.45

Table 8 Base shear (kN).

Earthquake	NC	1-TMD	1-EKD	2-TMD	2-EKD	3-TMD	3-EKD
Northridge	10645.0	9267.6	8765.7	9231.3	7742.3	9396.0	6821.5
L'Aquila	11385.2	11203.6	10719.1	11237.0	10262.1	11327.9	9716.6
Kocaeli	11193.6	8178.4	8378.4	7761.1	7184.1	7761.7	6195.1
Tabas	25543.8	23259.3	21592.2	23594.2	20306.4	23447.6	18815.4
Kobe	36296.1	25912.7	26053.0	25071.5	20910.1	24785.0	17633.8
Landers	13606.8	12705.3	12005.6	12594.9	11087.9	12572.5	10119.9
Duzce	2894.6	2668.3	2591.1	2603.1	2425.6	2533.4	2242.3
Friuli	8780.1	8392.7	7800.6	8244.6	7334.0	8219.8	7051.4